CHALMERS
UNIVERSITY OF TECHNOLOGY

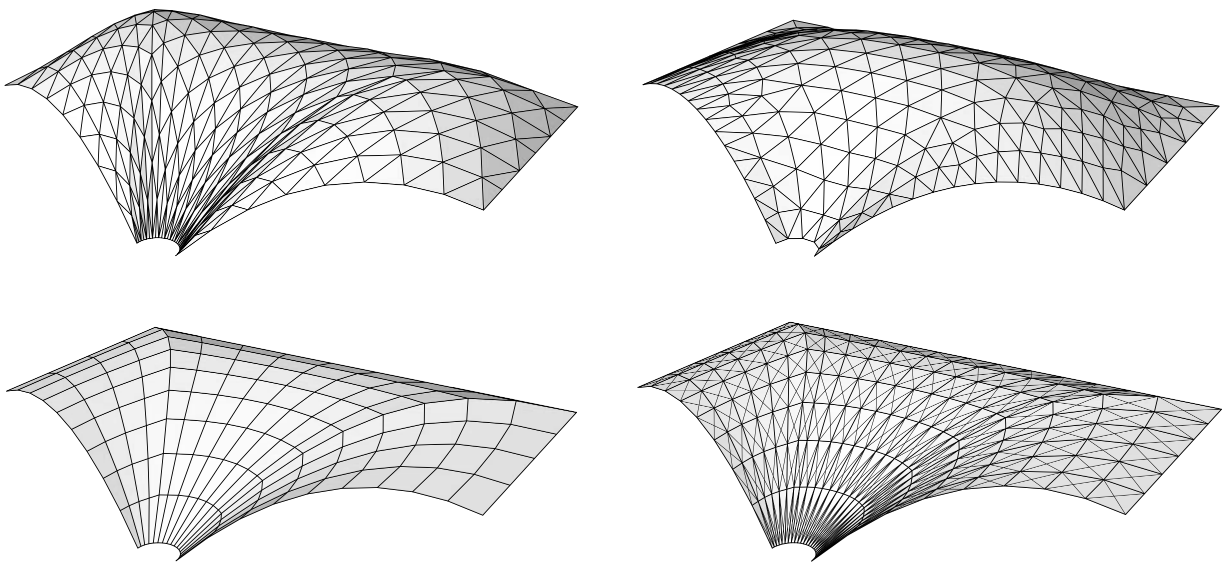

Rationalizing freeform architecture

Surface discretization and multi-objective optimization

Master's thesis in Structural Engineering and Building Technology

VIKTORIA HENRIKSSON & MARIA HULT

Department of Applied Mechanics
CHALMERS UNIVERSITY OF TECHNOLOGY
Gothenburg, Sweden 2015

MASTER'S THESIS IN STRUCTURAL ENGINEERING AND BUILDING TECHNOLOGY

Rationalizing freeform architecture

Surface discretization and multi-objective optimization

VIKTORIA HENRIKSSON & MARIA HULT

Department of Applied Mechanics
Division of Material and Computational Mechanics
CHALMERS UNIVERSITY OF TECHNOLOGY
Göteborg, Sweden 2015

Rationalizing freeform architecture
Surface discretization and multi-objective optimization
VIKTORIA HENRIKSSON & MARIA HULT

Master's Thesis 2015:94
ISSN 1652-8557
Department of Applied Mechanics
Division of Material and Computational Mechanics
Chalmers University of Technology
SE-412 96 Göteborg
Sweden
Telephone: + 46 (0)31-772 1000

Cover:
Different optimized solutions of a discretized surface

Chalmers Reproservice
Department of Applied Mechanics
Göteborg, Sweden 2015-12-18

Rationalizing freeform architecture
Surface discretization and multi-objective optimization
Master’s thesis in Structural Engineering and Building Technology
VIKTORIA HENRIKSSON & MARIA HULT
Department of Applied Mechanics
Division of Material and Computational Mechanics
Chalmers University of Technology

Abstract

With the help of modern computer aided tools, complex architectural shapes are becoming increasingly popular and easy to model and design. As a consequence, questions are raised of how to realize and produce the design in a feasible and affordable way. This issue, in the building industry, is known as rationalization. Today, this process normally takes place at the end of the design process, while if it is considered at an early stage, the greatest gains can be made.

In this study, rationalization in terms of different surface discretization methods has been a main focus. Geometrical theory of how to divide a surface into smaller elements have been studied for historical and modern buildings in order to understand what important factors exist. Site visits and interviews with practicing architects and engineers have been conducted in order to study different design approaches and rationalization of real projects. This study also explores multi-objective optimization, since most real design projects have several different aspects to consider when rationalization is performed. These are often more or less conflicting, resulting in many different solutions where trade-offs can be made in order to find a desired result.

The theory studied in this thesis is applied in a design project, where a new glass and steel gridshell structure is proposed. The structure is designed parametrically in the Rhinoceros® plugin Grasshopper® and structurally analysed with the FE add-on Karamba. Different possible solutions were investigated by the use of genetic algorithm optimization in the Grasshopper® add-on Octopus. The solutions are compared to each other in order to find an optimal solution regarding load bearing capacity, cost and architectural qualities.

The design project shows that the studied discretization methods have different advantages and drawbacks depending on the specific case. It also shows that the use of genetic algorithms and parametric design can be very effective for generating many different solutions to complex problems. However, the role of the designer is still very important when it comes to judging the result and selecting a design based on qualitative objectives.

Key words: Freeform architecture, Rationalization, Multi-objective optimization, Genetic algorithms, Parametric design, Finite element method, Form finding, Architecture and structural design.

Rationalisering av friformsarkitektur
Ytdiskretisering och multiobjektiv optimering
Examensarbete inom Konstruktionsteknik och byggnadsteknologi
VIKTORIA HENRIKSSON & MARIA HULT
Institutionen för Tillämpad mekanik
Avdelningen för Material- och beräkningsmekanik
Chalmers tekniska högskola

Sammanfattning

Komplexa arkitektoniska former blir allt mer populära och enklare att modellera och designa med hjälp av allt mer lättillgängliga datorprogram. Som en konsekvens till detta uppstår frågor om hur man kan realisera och producera dessa komplexa former på ett kostnadseffekt sätt. Detta område kallas ibland rationalisering. Idag sker denna rationaliseringsprocess ofta vid slutet av designprocessen, även om det skulle vara mer givande om det implementeras i ett tidigare skede.

Geometrisk teori över hur ytor kan delas in i mindre element har studerats för historiska och moderna byggnader med syfte att skapa en uppfattning om vilka faktorer som påverkar. Studiebesök och intervjuer med yrkesverksamma arkitekter och ingenjörer har utförts för att undersöka olika tillvägagångssätt inom designprocessen. Denna undersökning inkluderar också multiobjektiv optimering, då de flesta verkliga designproblem innehåller flera olika aspekter att ta hänsyn till vid rationalisering. Dessa aspekter kan vara mer eller mindre motstridiga, vilket resulterar i många olika lösningar där en avvägning genomförs för att hitta ett önskat resultat.

En metodik baserad på teorierna används sedan i ett designprojekt, där ett nytt glas- och ståltak för en innegård föreslås. Strukturen är parametriskt modellerad med hjälp av Rhinoceros®-tillägget Grasshopper® och sedan strukturellt analyserad med finita elementmetoden genom Karamba. Olika möjliga lösningar undersökts med hjälp av genetiska algoritmer, i optimeringsprogrammet Octopus inom Grasshopper®. Lösningarna är jämförda med varandra för att hitta en optimal lösning med hänsyn till konstruktiv kapacitet, kostnad och arkitektoniska kvalitéer.

Designprojektet visar att metoderna för att dela upp ytor har olika för- och nackdelar, vilket varierar från fall till fall. Det visar även att genetiska algoritmer och parametrisk design kan vara väldigt användbart för att generera många olika lösningar till ett komplext problem. Dock är designerns roll fortfarande avgörande när det kommer till att bedöma och välja en av dessa lösningar baserat på kvalitativa aspekter.

Nyckelord: Friformsarkitektur, Rationalisering, Multiobjektiv optimering, Genetiska algoritmer, Parametrisk design, Finita elementmetoden, Arkitektur och teknik.

Contents

Preface

This thesis comprises 30 ECTS and has been carried out during the autumn of 2015 at Chalmers University of Technology in Gothenburg, Sweden. The work was performed at the Department of Applied Mechanics with Dr. Mats Ander, senior lecturer at the division of Material and Computational Mechanics, as the main supervisor and examiner.

Our background with Bachelor of Science degrees in Architecture and Engineering has influenced the selected subject and the development and focus of the this thesis.

Acknowledgment

First of all we would like to thank **Mats Ander**, our supervisor and examiner for his enthusiasm, support and help throughout the process of this study. We would also like to thank **Karl-Gunnar Olsson** the founder of the Architecture & Engineering program for inspiring us through the education and funding our study and site visits.

Further we would like to thank **Jens Olsson, Martha Tsigkari** and **Francis Aish** at Foster + Partners for welcoming us to London to discuss their current project Mexico City Airport, and **Ulrika Davidsson** at Wingårdh Arkitekter AB for meeting us to talk about their built project Emporia Shopping Centre.

We would also like to thank **James N. Richardson** at Thornton Tomassetti in New York for his help and guidance through the optimization phase, and **Reza Haghani Dogaheh** for guiding us through simplifications of loads on freeform surfaces.

At last we would like to thank our opponent, **Emil Poulsen** for many rewarding discussions about form finding and surface discretization.

Göteborg December 2015

VIKTORIA HENRIKSSON & MARIA HULT

1 Introduction

In this chapter, the concept of freeform architectural surfaces is introduced. A brief historical overview of how the building industry has changed over time will be given and the aim, limitations and method of the thesis will be presented.

1.1 Background

The architecture and structural engineering industry have during the past decades undergone a digital revolution. Research on surfaces in geometric modelling took a big leap at the end of the 20th century, initiated by practical needs in the car manufacturing, aeronautic-, gaming- and animation industries (Pottman, et al., 2006). With the help of Computer aided design tools, complex architectural shapes can now be produced with minimal design input. As a consequence, freeform geometry is becoming increasingly popular among architects and structural engineers.

Even though freeform architecture does not have a proper definition, it is associated with smooth flowing shapes, often with both positive and negative curvature and lack of symmetries.

Complex geometries and freeform surfaces in architecture dates back to long before the modern computer-age. Some examples include dome-like shelters made from wood and willow, roman non-reinforced concrete domes or the early prismatic glass dome by Bruno Taut in 1914. It was only by the middle of 20th century, with the increasing popularity of reinforced concrete that architects and structural engineers really started to explore freeform shapes.

Figure 1.1 Left: Expo'58 pavilion Le Corbusier, 1958 (Photo: Wouter Hagens). Right: Sydney opera house, Jørn Utzen 1973 (Photo: Bjarte Sorensen). Both buildings got it's freeform shape realized by the use of reinforced concrete.

Before computers became commonly used, physical models were used in order to find the shape of a building as well as study the structural behaviour. Pioneer Buckminster Fuller, famous for his Geodesic dome, explored new possibilities for complex lightweight structures through mathematics and models. Other pioneers include Antoni Gaudi, with his catenary arch models, Frei Otto, famous for working and developing suspended structures, Hans Schober and Jörg Schlaich with their cable nets and gridshells as well as Heinz Isler through and his extremely thin concrete shells.

Figure 1.2 Left: Lightweight tent construction at the Munich Olympic stadium 1972, Frei Otto (Photo: btr). Right: Hippo House, Berlin Zoo, 1996. The freeform surface is covered with planar quadrilateral glass panes (Photo: Schlaich Bergermann Partner).

As freeform shapes emerges more often, questions are raised concerning realization and production of complex designs in feasible and affordable ways. This issue, in the building industry, is known as rationalization. The tools used in architectural design were originally developed for industries with a difference in scale, aesthetics and manufacturing techniques, making rationalization even more crucial.

Figure 1.3 Milan Trade Fair glass roof by Schlaich Bergermann Partner. The mesh grid of the freeform glass roof flows seamlessly from the quadrilateral mesh (flat top region) to the triangular one within the funnel region (Photo: Ramon Prat).

Today, freeform architecture can be found almost all over the world. Architects such as Zaha Hadid, Sir Norman Foster and Frank Gehry all contribute to the modern freeform architecture. These freeform shapes are not yet very common in Sweden and the rest of the Scandinavian countries. However, examples such as the Emporia Shopping Centre and the Triangle station, both in Malmö, have been built in recent years.

The process of rationalizing freeform surfaces normally takes place at the end of the design process, while if it is considered at the initial stage, the greatest gains can be made. This report will study different ways of rationalizing freeform architecture based on a set of criteria. It will explore how for example the structural behaviour and architectural aesthetics will influence the chosen rationalization method.

1.2 Aim

When rationalizing a freeform surface, many different aspects can and need to be considered. The purpose of this thesis is to investigate different methods of rationalization of freeform architectural shapes into buildable structures, and to investigate which factors influence the constructability and cost of the final structure.

The aim is to apply this theory on a study project in order to investigate the rationalization process, in which a freeform surface will be studied from initial sketch to conceptual design solutions. The aim for this design is to not only be structurally optimized, but take other aspects under consideration such as original design intent, simplicity of design, material usage etc. though multi-objective optimization.

The purpose of this thesis is also to explore how existing computer tools can be utilized in a design method when working with freeform architectural shapes.

1.2.1 Thesis questions

- How can a freeform architectural shape be rationalized?
    - What aspects does the term rationalized contain?
    - What are the most important aspects?
- How will different discretization methods affect the structural behaviour?
- How can the rationalization method be implemented in the design process?

1.3 Limitations

Some types of structures, for example concrete shells, inflatable structures and timber gridshells, will not be studied in depth.

The focus for the study project will be on the overall structure, and therefore it will not be solved in a detailed scale. Effects such as long term creep and temperature loads will not be considered.

Already existing commercial softwares will be explored and combined instead of creating new programs. Different kinds of genetic algorithms and FE-modelling programs will not be studied, but the study will be conducted within Grasshopper® and its add-ons Octopus and Karamba.

1.4 Method

In order to get a better knowledge of the subject, literature studies will be conducted as a starting phase. This includes identifying different methods of discretization of freeform surfaces such as triangular and quadrilateral division, gridshells and tensile structures. Already built examples around the world will also be studied and for some projects, site visits will be conducted. Architectural and engineering offices in Sweden and abroad will be visited to discuss how freeform projects can and have been rationalized. The theory of single and multi-objective optimization will also be studied. Different optimization criteria will be identified along with the evaluation of the different discretization types.

The study project that will be designed is a mean of exploring the rationalization process, existing design tools and evaluation criteria. This project will be a canopy at the courtyard of the civil engineering building at Chalmers University of Technology. A design program will be specified where boundary conditions are stated. Further, an initial design will be developed through sketches and model making. The most promising methods of discretization will be compared and developed through the use of multi-objective optimization with genetic algorithms. This process searches for structurally and material efficient solutions that also take aesthetic qualities under consideration. One individual is selected for each of the four chosen discretized surfaces. They are then compared and further rationalized.

The process will be explored through computational and physical sketch models. The softwares that will be used are Rhinoceros® and its plugin Grasshopper® with add-ons Octopus, Kangaroo and Karamba.

2 Surface theory

The following chapter contains theory of structural stability and form finding. It also introduces different methods of surface realization together with built examples.

2.1 Structural stability and form finding

For a structure to be statically stable, it needs to be in equilibrium with the external forces it is subjected to. The overall geometry of a structure is of high importance during the design process. The priority of the functionality and aesthetics of the geometry can vary between different design projects, but a combination of both is preferred in most cases. Structures working in tension and compression is more efficient when it comes to material usage and lowering the deflections compared to structures working mainly in bending.

Form finding in structural engineering and architecture is often used to describe the act of finding the shape of a design such that is works in mainly tension and compression. The governing load used for form finding is usually the structures self-weight, but it can also be other external loads.

Historically, the importance of finding a shape that works mainly in compression was essential, as traditional construction materials such as masonry and stone only resist small tensile stresses. The traditional arches and domes are some of the first form found structures, which got their shapes with help from the hanging chain principle. By inverting the shape of a hanging chain, which works in pure tension and is free from bending, a pure compression structure will be found. Later, in the 20's century investigations through physical models using hanging cloths, soap film and chain networks were conducted.

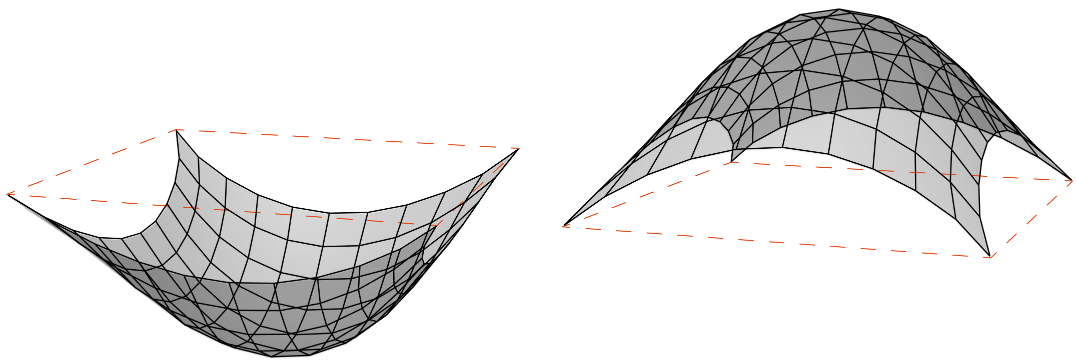

Figure 2.1 Form found surface according to a catenary curve shape. Hanging shape working in pure tension (left) and inverted shape, giving a form that mainly works in compression (right).

Today, with the help of modern computer programs, different kinds of numerical methods can be used for form finding. One type of these are the geometric stiffness methods, which are material independent. A particular example of this is the Force Density Method, which is based on the ratio of force to length. Other methods include dynamic equilibrium methods, for example Dynamic Relaxation, which results in a geometry where all forces are in equilibrium through iterations in small time steps. Another way to find a shape is through large deformation analysis using the finite element method (Veenendaal & Block, 2014).

An important factor for a structure to be globally stable, is the support conditions. A way to technically describe this is by the degrees of freedom (DoF). For static structural calculations, DoF is the number of independent movements a body has. In a three dimensional space, an unrestrained body has six degrees of freedom; three translational and three rotational. The translational DoF's represents the movement in three perpendicular axes (usually x,y,z), similar is the rotational DoF's which represent the rotations about these axes.

In order for a structure to avoid moving around freely in space (rigid body modes), it needs to be restrained for these movements at the supports.

2.2 Gaussian/Principal curvature

When discretizing freeform surfaces, particularly when laying out flat and single curved panels, studying the curvature behaviour is essential. One way of measuring the curvature of a surface is by the Gaussian curvature, which is a scalar that is the product of the two principle curvatures. The two principle curvatures, k_1 and k_2, are the maximum and minimum curvatures which are perpendicular to each other. The Gaussian curvature is expressed as $K = k_1 \cdot k_2$ at every point on the surface.

A geometric way of specifying if the Gaussian curvature is positive, negative or zero, is by studying the direction of these principle curves. Principle curves with the same sign, as for a dome, will have a positive Gaussian curvature. For a hyperboloid where the principle curves have different signs, the Gaussian curvature is negative. For a single curved surface, the principle curvature in one direction is zero, making the Gaussian curvature zero. The sign of the Gaussian curvature is of importance when mapping panels on a surface, particularly for hexagonal grids which will be explained further in the this chapter.

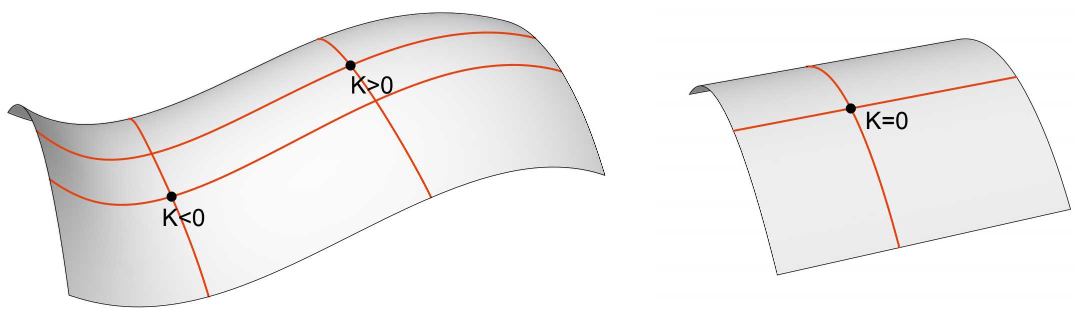

Figure 2.2 Principle curves and Gaussian curvature on surfaces.

2.3 Surface discretization

There are different ways one can realize freeform surfaces, one common way is to divide it into segments, commonly known as discretization. Discretization can be done in a lot of different ways, some of which will be explained in this chapter. The discretization methods vary in number of element face edges, node complexity, face curvature, material suitability etc. For example, planar elements are often preferred since production costs generally are lower than for curved elements. Often, for curved elements, a unique mould has to be created for each element. Since the moulds often can be more expensive than the element itself, this results in an expensive solution.

This chapter will cover triangular, quadrilateral and hexagonal meshes, and some examples of how different shapes can be combined will also be presented. Different methods are of course suitable for different cases, but a general explanation and advantages/disadvantages will be stated below. Built examples of each method will be given. As a last part of this chapter, other methods to realize freeform surfaces will be presented shortly.

2.3.1 Triangular meshes

Triangulation of surfaces is a common way to discretize a surface. A triangular mesh has the advantage of always creating flat panels between three points. This way, a planar triangle mesh can approximate any given surface. The disadvantages however are that a triangular mesh results in a high number of elements and high node complexity since typically six edges meet in each node. These disadvantages also often results in low structural transparency, which can be a problem when working with a see-through covering material such as glass.

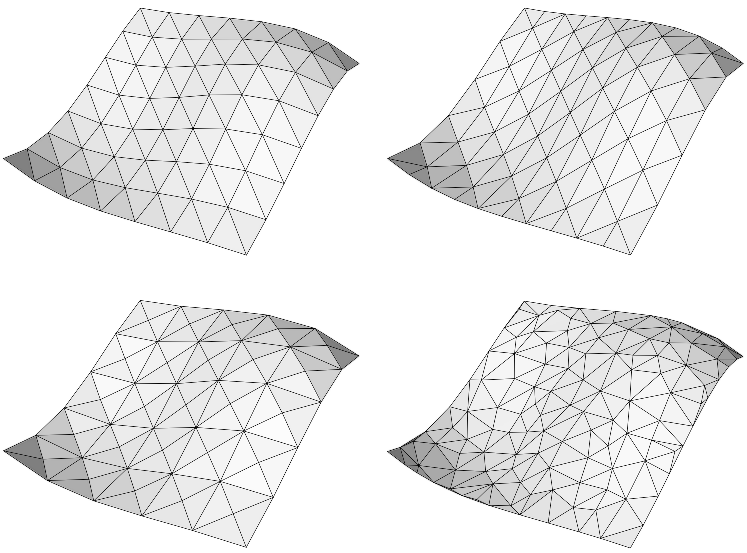

Figure 2.3 Different ways of triangulating a surface, all with a unique architectural expression.

One problem with a triangular mesh is that an exact offset mesh cannot be created for any arbitrary surface. This can cause issues for the layout of supporting beams and multi-layer meshes. When offsetting a triangular mesh, the individual triangles become scaled versions of one another. Therefore only near-spherical or plane meshes can be offset at a constant distance. An approximated offset mesh for a freeform surface will have an error distributed over all the nodes (Pottman, et al., 2006).

There are many possible ways one can triangulate a surface, making it relatively easy to adjust the mesh to fit the force paths. Compared to other discretization methods, where one will need to follow more strict mathematical rules in order to subdivide the surface, triangular meshes have larger possibilities for structural optimization. In order to create a structurally efficient design, the design must be able to transfer the loads favourably, with minimal bending, through membrane forces (Schlaich & Bergermann, 2005). A triangular grid is particularly good in this aspect, where each element is stable for in-plane forces. This makes it possible to use hinged connections between the structural members.

One well-known example of a triangulated steel grid is the roof over the Great Court of the British Museum in London. The grid was created using form finding and in total the roof consists of 3 312 unique panels of glass. Half of the elements are though a mirrored copy of another as the courtyard is symmetric along the north-south axis. A triangular structural grid was chosen because of its structural efficiency and the fact that a triangular mesh always creates flat faces (Williams & Shepherd, 2010).

Figure 2.4 The Great Court of the British Museum in London is covered by glass with a triangular steel mesh. It was opened in 2000 and designed by Foster + Partners and Buro Happold.

2.3.2 Quadrilateral meshes

A quadrilateral mesh has several advantages over a triangular mesh. The mesh has a smaller number of edges which often results in less use of structural material, lower node complexity and a higher structural transparency. According to (Schober, et al., 2002), quadrilateral meshes are by far easier to manufacture compared to triangular meshes, due to the fact that they require less mullions and machining operations. However, a quadrilateral mesh does not automatically have planar faces as for a triangular one. Therefore, quadrilateral meshes are sometimes made of single or double curved elements, but as mentioned above, this is a more expensive solution. The three types will be explained below.

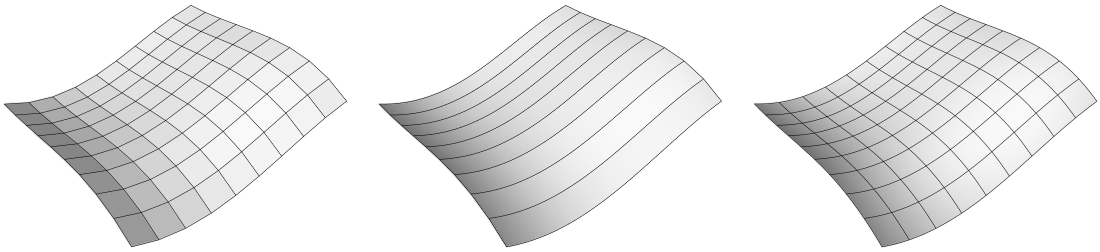

Figure 2.5 *Different ways of subdividing a mesh with quadrilateral elements, a mesh with planar faces (left), single curved elements (middle) and double curved elements (right).*

In order for quadrilateral meshes to be stable for in-plane forces, the face material can be utilized or additional diagonal members can be added. Moment connections can also be used, which are much more complex and expensive to construct compared to hinged connections.

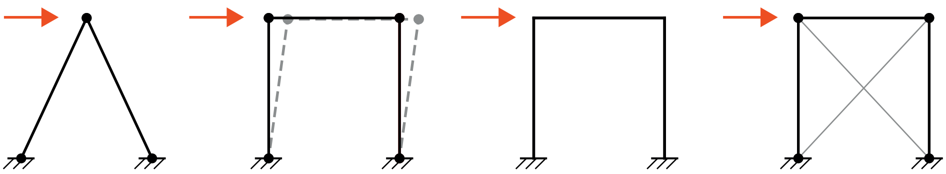

Figure 2.6 *Structural stability of triangular and quadrilateral meshes. The two figures to the right shows two ways of stabilizing quadrilateral meshes, either by stiff connections or diagonal members/face material.*

2.3.2.1 Planar quadrilateral meshes

A quadrilateral mesh with planar faces (PQ mesh) is an approximation of the initial surface. Planar faces are preferred especially when working with materials that are expensive or even impossible to bend. Since a PQ mesh cannot be constructed on any arbitrary freeform surface, the original surface may have to change to be able to fit a PQ mesh. However, in some cases small changes in the overall geometry can be preferred to attain the advantages that it has over a triangular mesh.

Another advantage for PQ meshes is that, according to (Pottman, et al., 2006), the higher number of edges in a planar face, the easier it is to create an offset mesh. Therefore, a PQ mesh is often a better option than a triangular one when it comes to multi-layer meshes and to reduce the torsion in the nodes for the supporting system.

Hans Schober, partner of Schlaich Bergermann Partner, developed a strategy for generating quadrilateral planar facets of double-curved surfaces. The method is based on the principle that two parallel vectors in space always define a planar quadrilateral surface (Schober, et al., 2002). With this method, two of the four sides of the quadrilateral mesh will be parallel, either the longitudinal- or the lateral edge.

Schober's method includes two ways of generating a special surface, the first way is the "Translational surface". It is created by translating any special curve (generatrix) against another random curve (directrix). Subdividing these curves equally will create a planar mesh with constant bar length. Another surface fit for planarization is the “Scale-Trans-Surfaces”, which is created in a similar way as the “Translational surface” with the difference that the generatrix curve is scaled and translated against the directrix.

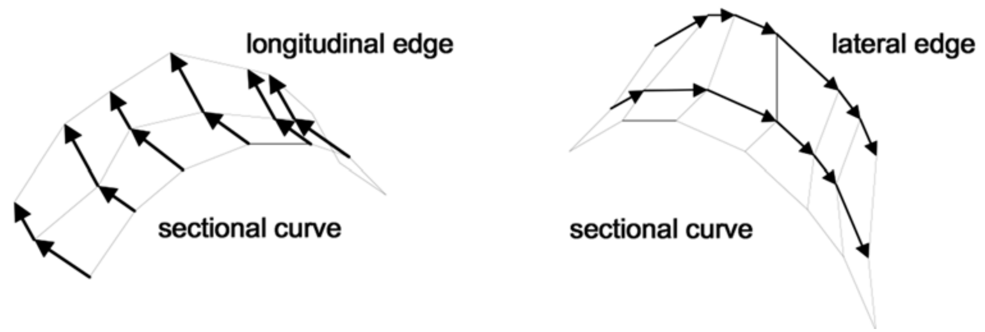

Figure 2.7 *Basic principle for planar quadrilateral meshes. Left figure shows parallel longitudinal edges while the right figure shows parallel lateral edges (Image: Hans Schober).*

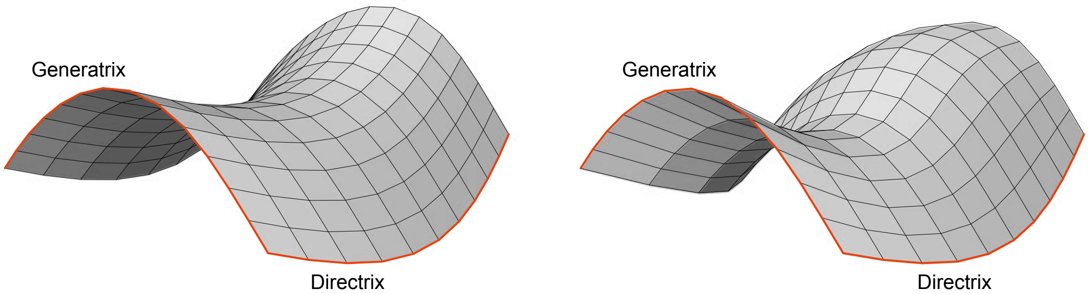

Figure 2.8 *Example of Translational surface (left) and Scale-Trans-Surface (right).*

Figure 2.9 *Glass roof at the Museum of Hamburg History, GMP Architects and Schlaich Bergermann Partners. The glass roof consists of flat glass panels, with diagonal cables creating required stiffness (Photo: Heiner Leiska).*

Two other methods of discretizing a surface with planar faces, is by using a ”Conical” or ”Circular mesh”. The circular mesh can be understood as a quadrilateral mesh where all vertices of a face are positioned on a flat circle on the surface. This method is particularly good since the opposite angles for a quadrilateral inscribed in a circle are supplementary, meaning that the two angles will add up to 180 degrees. This means that the created quadrangle is close to a rectangle with each angle approximately 90 degrees.

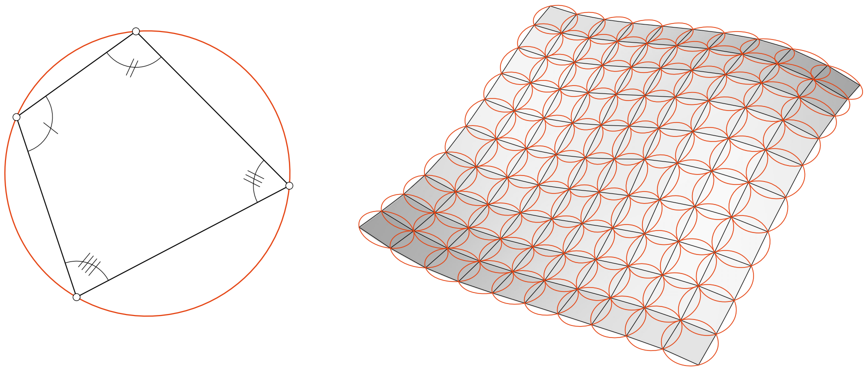

Figure 2.10 Left: A quadrilateral inside a circle, the sum of the two opposite angles is 180°. Right: How a circular mesh is fitted on a surface, making planar quadrilateral elements.

A surface can also be divided along the principle curvature lines. A vector field is created over the surface and connected into lines. An advantage with a principle curvature quadrilateral mesh is that since the principle curvatures are perpendicular to each other in each point, the quads will be close to rectangles when the lines are straightened out in-between the points. According to (Zadravec, et al., 2010), a mesh based on principal curves on a surface is often close to have planar faces. A drawback of the method is however that depending on the surface, the spacing between the curves can be uneven, meaning the panels can differ much in size.

In a computational environment, a discretized surface can be given a set of both material-realistic and pseudo-physical properties. The pseudo-physical properties do not actually exist, but make the element react in a physical way to forces applied to it. This way, realistic or forced physical behaviour can be simulated, to achieve planarity of faces, equal size elements etc. This method can therefore be used for creating a PQ-mesh, but is also applicable for other element face shapes. A tool for simulating physical behaviour is the Grasshopper add-on Kangaroo, which will be described more further down in this chapter.

2.3.2.2 Single curved quadrilateral meshes

It is also possible to divide a surface into single curved elements. These are often less expensive to produce than double curved ones and can give a closer approximation of the original shape than planar elements. However, bent panels are still more costly than flat ones, but can be a good compromise.

A surface can be developed into single curved strips by first creating a PQ mesh according to one of the methods described in section 2.2.2.1. One strip of planar quadrilaterals can be unfolded into the plane. If this strip is refined into infinitely many elements and the planarity of the elements is kept, a developable strip (D-strip) is generated, and can still be unfolded into the plane without stretching or tearing (Pottman, et al., 2008).

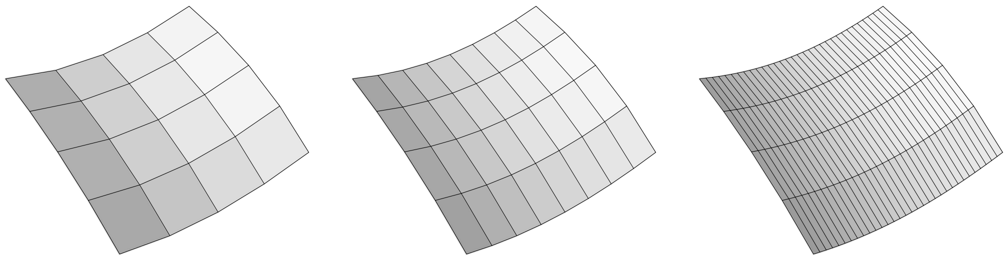

Figure 2.11 Single curved elements can be created out of a planar quadrilateral mesh by refining the strips into infinitely many quads.

The strips can be manufactured by bending instead of using moulds. This is especially suitable for materials such as metal sheets that are easily bent in one direction into a desired shape. One example of this is the Guggenheim Museum in Bilbao by Frank Gehry, where the double curved façades are built up by single curved sheets of titanium, see Figure 2.12. Gehry originally designed the building by gluing physical stripes of paper, enabling the surfaces to be constructed with single curved elements held up by a lattice grid in structural steel (Nero, 2004).

Figure 2.12 The Guggenheim Museum in Bilbao by Frank Gehry is covered with single curved titanium sheets.

2.3.2.3 Double curved quadrilateral meshes

Double curved panels are sometimes desired because of their ability to create a surface that is identical to the initial surface, instead of being an approximation. A surface with double curved elements is smooth and not facetted as for one with planar elements. For a surface with high curvature, a mesh with planar elements could distort the appearance or even be impossible to create.

One example of a building with double curved glass elements is the Hungerburgbahn in Innsbruck, by Zaha Hadid Architects where separate moulds has been created for each panel (Eigensatz, et al., 2010).

Figure 2.13 Left: Hungerburgbahn in Innsbruck by Zaha Hadid Architect (Photo: Hafelekar). Right: Kunsthaus in Graz by Peter Cook and Colin Fournier (Photo: Schneider & Aistleitner). In both buildings, a separate mould for each element was used.

In order to have a more efficient manufacturing process for double curved elements, one can try to reduce the number moulds or have less complex moulds. This can be done by finding symmetries so that the moulds can be used more than once or finding pieces of the surface that can be made out of more simple moulds such as cylinders, paraboloids, torus patches etc. (Eigensatz, et al., 2010).

2.3.3 Hexagonal meshes

Another way to discretize a surface is using a hexagonal mesh. Since node complexity is a major factor in manufacturing cost, a hexagonal mesh has some advantages over a triangular or quadrilateral mesh, where only three beams are joined at each node. However, while a planar hexagonal mesh (P-Hex mesh) is suitable for some special shapes, such as constant mean curvature surfaces, it can be very hard and sometimes impossible to fit a P-Hex mesh onto an arbitrary freeform surface and at the same time prevent the mesh to self-intersect (Wang & Liu, 2010).

Sometimes other geometrical shapes are needed to help cover the surface with a P-Hex mesh. Pentagons are a common alternative. One well known example of such a closed surface, with genus 0, is an ordinary football, that consists of 12 pentagons and 20 hexagons. Only a closed surface of genus 1 can be covered with only planar hexagons (Wang & Liu, 2010). One example for this is a torus.

Concave hexagons is created for surfaces with negative Gaussian curvature, such as the inner circle of the torus or hyperboloid, which may not always be aesthetically desirable.

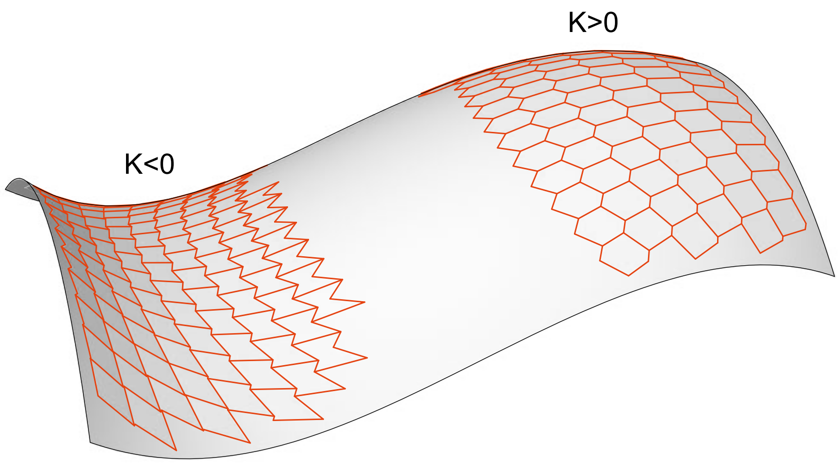

Figure 2.14 Planar hexagons on a surface. The hexagons are convex where the Gaussian curvature is positive, and concave at negative Gaussian curvature.

Similar as for a quadrilateral mesh, the hexagonal mesh also needs either connections that can transfer moment or additional structurally stabilizing members in order to be structurally stable. The domes of the Eden Project consist of hex-tri-hex space frames in two layers, see Figure 2.15 (Eden Project, 2001). Even though the inner layer does not consist of only triangles, the layers work together and stabilize the shell.

Figure 2.15 Eden Project in Cornwall by Grimshaw Architects and Anthony Hunt Associates. Eight large inter-linked domes create humid and temperate regions. The structure is covered with triple-layered pillows of ETFE foil, which was used instead of glass to create a light-weight roof structure (Eden Project, 2001).

2.3.4 Combination of different geometrical shapes

In some cases, different shaped panels can be used out of structural or aesthetic reasons. In the large glass and steel structure of Milan Fair both quadrilateral and triangular panels were used, see Figure 1.3. The surface was primarily designed as a triangular mesh and were then generated to a quadrilateral one. Thinner rods were then inserted in all places where the elements were not planar, creating planar triangles (Schlaich Bergermann Partner, 2005). This way, there is less use of material in parts where it is not needed.

Another example of a surface where quadrilateral and triangular elements are mixed is the Department of Islamic Arts at the Louvre in Paris. The mission was to make a triangulated mesh structure more lightweight by making it into a PQ mesh. This was however not possible to design without changing the boundaries too much and did therefore not meet the architect's idea. A mesh with both triangles and quadrangles was therefore made, and it was easier to meet the intention of the initial surface (Pottmann, 2014).

The glass roof over the courtyard of the Scheepvaartmuseum in Amsterdam, which was added during the renovation of the museum in 2011, is another example where the surface is divided into different shaped elements, see Figure 2.16. The geometry is set by lines passing from one edge of the surface to another, creating a pattern that is found on historical Dutch nautical maps preserved in the museum. The shape of the dome was decided by the maximum height of the surrounding building and to achieve material efficiency. The grid divides the roof into triangles, quadrangles, pentagons and hexagons, all planar glass panels. As a result of the intersecting pattern, the panels differ a lot in size and more than 6000 different steel elements are used (NEY+Partners, 2011).

Figure 2.16 Left: Area where triangles turn into quadrilateral panels at the New Milan Trade Fair (Photo: Studio Fuksas). Right: The new glass roof at the Scheepvaartmuseum, designed by the architect and civil engineer Laurent Ney.

2.4 Other methods of surface realization

Freeform architectural surfaces are not only created by dividing the surface into geometrical shapes as described above. There are several other methods to accomplish such shapes.

Concrete is easily shaped by casting, where the difficulties and costs lays in the casting moulds and the reinforcement design. Concrete shells can be expressed in significantly freeform flowing surfaces such as The Ocenographic in Valencia by the architect Félix Candela and structural engineer Alberto Domingo, see Figure 2.17 (left). The concrete roof is form found in order to find a structurally efficient shape, similar to the work of Heinz Isler.

Traditional materials such as stone and masonry has also been used to realize modern freeform structures, particularly structures working primarily in compression. The Mapungubwe Interpretation Centre in South Africa is one example of this, made from un-reinforced bricks, see Figure 2.17 (right).

Figure 2.17 Left: Thin concrete shell roof at the L'Oceanogràfic in Valencia by Félix Candela (Photo: Felipe Gabaldón). Right: Masonry shell at Mapungubwe Interpretation Centre, Peter Rich Architects (Photo: Iwan Baan).

Another type of a freeform stucture is the timber gridshell. A timber grid can be created in the same way as a steel grid with straight beams that are cut off and connected in each node. More commonly, timber gridshells are created by a net of long slender interwoven laths that are laid out flat and then bent into its final shape. The final grid structure therefore consist out of curved members and create curved spaces in between, see Figure 2.18 (left).

Figure 2.18 Left: Weald and Downland Gridshell by Buro Happold and Edward Cullinan Architects (Photo: Hugh Chevallier). Right: TRADA pavilion by Rambøll Computational design (Photo: Rambøll).

A way to divide a surface into different shaped cells is with a Voronoi diagram. This can be created from a specified set of points on the surface, where each point will have its own region. Depending on where the surface points are created, the regions will differ a lot in shape and size, see Figure 2.19 (right). This may not be a rational way of discretizing a surface, but it can however give a good approximation for planar elements on a surface since smaller ones can be applied where needed in areas with high curvature.

Figure 2.19 Left: Membrane roof over Urban-Loritz-Platz in Vienna by Silja Tillner and Schlaich Bergermann Partner. Right: Ontario's Celebration Zone for the Pan Am and Parapan Am Games in Toronto by Hariri Pontarini Architects, Thornton Tomasetti and Blackwell.

Another example of constructing freeform shapes is by using membranes. A special type of membrane structure is an inflatable one where a surface is created out of a cutting pattern and structurally held up by "air beams", see Figure 2.19 (right).

3 Design and Optimization

Rationalization of the design process can be just as important as rationalization of the design. Depending on how a design problem is approached, the result can differ. The following chapter introduces an overview of how the design process can be conducted. It also explains two different design approaches form a theoretical and professional application point of view. The chapter also contains optimization theory and explanation of different computer programs and how they can be used in a parametric design process.

3.1 Design approach

Two different ways of approaching a design task is the top-down and the bottom-up approach. The top-down approach is sometimes called stepwise or decomposition approach. It starts with the overall picture in mind which is broken down into sub-systems/more refined levels. The top-down approach is said to have been followed at École des Beaux-Arts school of design, where it was taught that an architecture design should begin with an overall plan and processed by stepwise refinement (Mitchell, et al., 1988). This approach allows for bigger teams to work on different parts of the project, which are easy to combine.

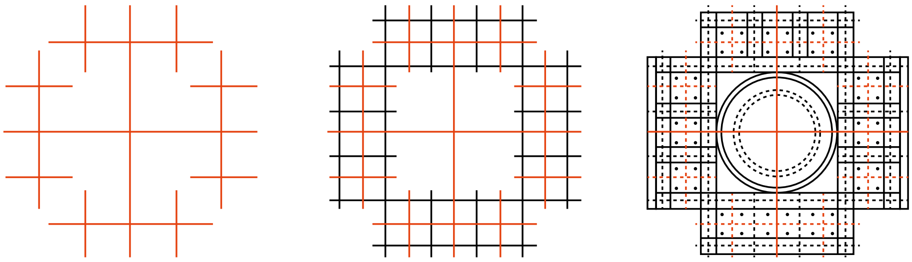

Figure 3.1 Stepwise refinement of a schematic plan into a detailed floor plan redrawn from sketches made by J.N-L. Durand (Mitchell, et al., 1988).

Bottom-up however, is an approach where the system is put together by individual elements that are linked together until a complete top-level system is formed. An easy understandable example of the bottom-up approach is a Lego-design where many different Lego parts are linked together to form a global shape.

Figure 3.2 shows how these design approaches can be described for a freeform surface design task. A good way of designing could be to combine the two approaches. A strength of the top-down approach is that a clear and simple vision can be followed all the way through the design, but sometimes the design can be too specified for detailed systems to fit in the end. The bottom-up approach can give a great freedom of designing the individual parts, but can lead to problems when putting the parts together and perhaps create a too complex result.

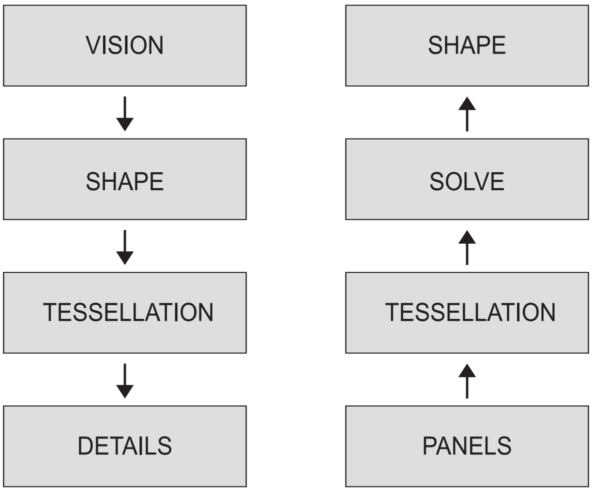

Figure 3.2 *Flow-chart of the top-down (left) and bottom-up (right) design approach, if the approaches were to be applied in a freeform surface discretization design problem.*

3.1.1 Professional application

Different architectural offices approaches a design in different ways. During an investigation of how real offices work with rationalization in early and later stages of the design, two architectural companies were visited; Wingårdhs in Gothenburg and Foster + Partners in London.

Wingårdhs is one of the most prominent architectural offices in Sweden and are known to work artistically, conceptually and design out of the ordinary. They have designed one out of only a few buildings with freeform features in Sweden, the Emporia Shopping Centre in Malmö, see Figure 3.4. The building has two freeform glass surfaces at the two main entrances, one with the colour amber and one sea blue. The intent of the shape is to create an exciting entrance and to draw people into the building. The amber coloured surface is created of 473 unique double curved glass panels and has a diagonal basket-like supporting structure that can be seen behind the glass (Davidsson, 2015).

Figure 3.3 *Left: Rendering of the initial design (Image: Wingårdh Arkitektkontor AB). Right: Finished building (Photo: Tord-Rikard Söderström).*

Wingårdhs' design approach for Emporia can be called a top-down approach. The final surface is very similar to the initial design at the competition stage, see Figure 3.3, keeping the original vision all through the project. According to Davidsson in an interview in October 2015, they were more or less determined from the beginning to use double curved glass to reach an almost seamless, flowing surface. Investigations were made to see how it could be done with for example flat triangles, but it did not meet the architects aesthetic demands. The diagonal division of the surface was made by the architects to create a dynamic flow, but the detailing and construction was made by the Spanish steel contractor Folcrá. Wingårdhs wanted the glass panels to be as big as possible to reach a high transparency, the maximum height was thus set by the furnace used by the glass manufacturer Cricursa (Davidsson, 2015).

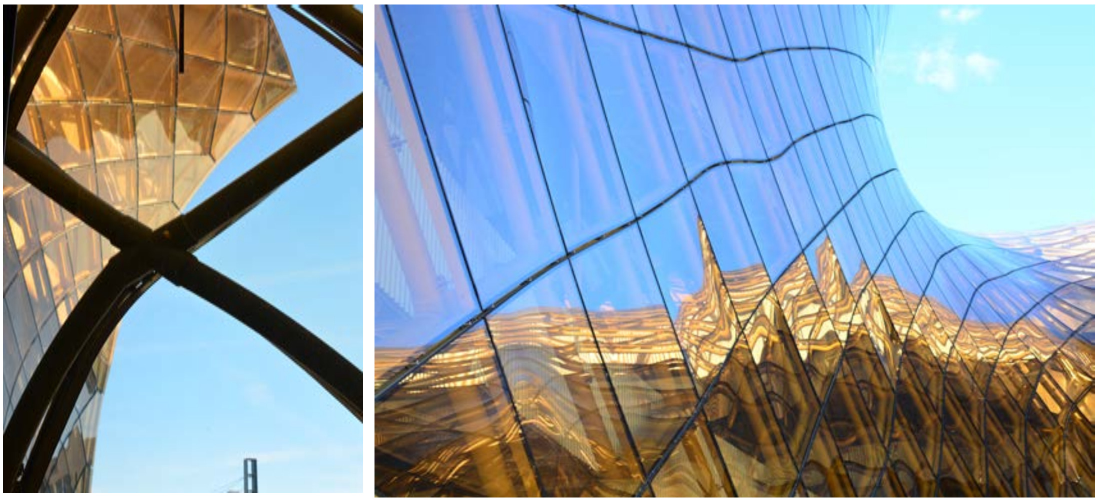

Figure 3.4 *Double curved glass panels of the Emporia Shopping Centre entrance. The maximum size of the panels are 2x4,5 m. The glass panels consist of 2x8 mm laminated glass.*

During a site visit to Emporia Shopping Centre in October 2015, a few questions regarding rationalization arose. The supporting system has curved elements with large dimensions to support the glass panels. By allowing the seemingly arbitrary surface to change, there might have been greater possibilities to create a more slender structure which also would increase the transparency. As can be seen in Figure 3.4 (right), the seams between the panels are not flowing continuously in all areas, and appear crooked from some angles. Even though surface discretization has not been a major focus for the surface itself, rationalization of the building process has. The smaller (sea blue) entrance surfaces is created out of the larger (amber) one, making it possible to reuse a large amount of the moulds and thereby reducing the cost substantially compared to having two completely different surfaces.

The next office visited, Foster + Partners is a renowned architectural office working with projects all over the world. They have an integrated design process where architects and engineers work together from the very beginning of their projects. A project of interest in this study is the ongoing New International Airport in Mexico City (MCA). Foster + Partners London office was visited in November 2015, to talk about the project and their design process.

The airport is going to be one of the largest in the world where the main structure of the building is a smoothly shaped roof, enclosing the terminal with an approximate surface area of 500 000 square meter, see Figure 3.5. The roof is flowing continuously to fulfil the vision of *one experience* and to connect all the different parts into one. The roof (in the stage it is in now) is defined by a two layer triangulated space frame structure with maximum spans of up to 170 m. All vertical loads are being transferred along the perimeter and through vertical supports (funnels) that are integral part of the space frame geometry. In order to create a structurally efficient design, the shape is intended to follow a catenary curve, slightly adjusted in order to accommodate spatial internal and external constrains (Olsson, et al., 2015).

Figure 3.5 MCA overview and interior visualization (Image: Foster + Partners).

MCA is a strongly integrated project, as the design team has been working with the engineering office Arup since the start, as well as with in-house engineers at the competition stage. Detailing is always an important factor for Foster + Partners, making sure to have full control over the design. Their choice of geometry in MCA – a triangulated space frame – is motivated by the structural efficiency of bars working mainly in tension and compression. They are continuously working with the mesh to find the visually most pleasing balance between bar length, profile size and bar position. They investigate manufacturing capabilities early on to see what is actually possible to accomplish (Olsson, et al., 2015).

These constrains combined with an overall design idea, where form finding has been performed, is an example of the use of the bottom-up approach together with the top-down one. The limitations are not seen as a hindrance, but as a framework for a design that guaranties a final product that is realizable. This way of working can create a shape that is optimized with respect to both global structural efficiency and manufacturing possibilities.

Figure 3.6 MCA interior visualization. The vertical supports (funnels) are integrated with the roof (Image: Foster + Partners).

In this project, Foster + Partners have strived to develop an efficient design. Efficient in terms of structure but also in terms of reducing the costs, for example by minimising the amount of material used and the complexity of junctions. The amount of different types of elements can be a factor, but its significance depends on the contractor's methods. Still, the number of different panels have been limited whenever possible, by rationalising parts of the space frame.

The two architectural offices visited have very different work strategies, much depending on what they aim for as a final result, but also the knowledge within the office and the working culture and practice in the different countries. At most architectural offices in Sweden, engineers are traditionally and usually involved relatively late in the design process, whilst at Foster + Partners the aim for all projects is to integrate structural and environmental design early on. Many architectural projects are becoming more and more complex, where a big task is to combine all different aspects.

The structural engineer Ove Arup, known for working very closely with architects, has over the years pointed out this change in roles and the need for the various stakeholders to understand each other in order to contribute to the overall design. The expression 'Total Design', stated by Arup is often used to describe this point of view where the education becomes an important factor (Grange, 1998). The need for knowledgeable architects and engineers in their respective fields are very important, but the ability to see and understand the whole picture is equally important. Technically skilled architects have the knowledge that can make it possible to relinquish traditional solutions, and instead create new innovative designs. This is equally true for engineers with architectural skills.

3.2 Generative design & optimization

Parametric or generative design has played an important role for modern architecture, giving the possibility for the designer to explore multiple design options in a fast way. According to Lars Hesselgren, one of the founding directors of SmartGeometry Group, generative design is not about designing a building. It is about designing the system that designs the building (Hesselgren, 2009). Initial parameters are defined and linked together under certain rules to form a system from which a design result is generated normally using a computer program. By changing the initial parameters, the design result changes accordingly, making generative design a very powerful tool, particularly in an initial design phase. Parametric modelling makes it possible to change the design, without redrawing everything all over again.

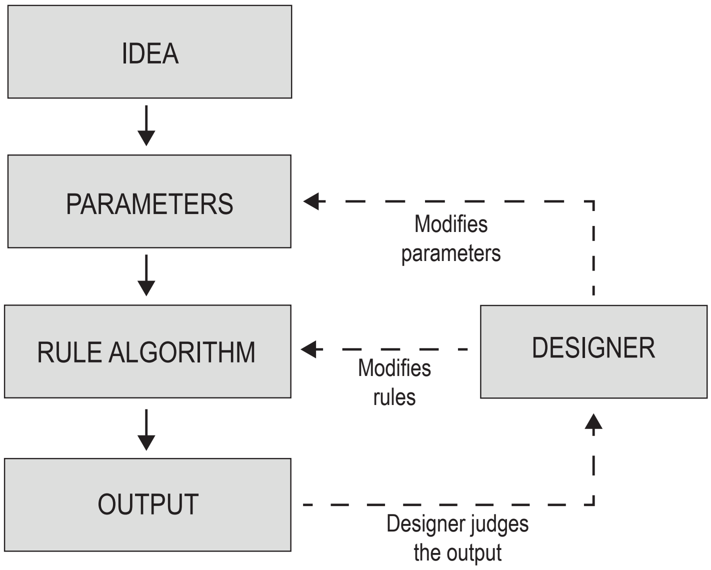

Figure 3.7 Flow chart over a parametric process.

By implementing structural analysis and optimization into the parametric environment, the designer can quickly evaluate the performance of the design. Adjustments to the initial parameters can then be made and the results will all change accordingly.

The central aim of optimization is to search for the best solution, according to an objective function, often called fitness function, containing one or several objectives. Usually it means targeting one or multiple objectives, subject to certain constraints, and minimizing them until they reach optimal solutions. This can be written as:

$$\begin{cases} \text{min} & \left(f_1, f_2, \dots, f_{n_f}\right) \\ \text{subject to} & \text{constraints} \end{cases} \tag{3.1}$$

where n_f denotes the number of objective functions, f_i:s, considered (Sehlström, 2013).

3.2.1 Multi-objective optimization

In practice, many real design problems have multiple competing objectives, both regarding engineering and architectural aspects. These are often in different degrees conflicting, resulting in many possible solutions which are not optimal for all functions. There are different ways one can solve an optimization problem containing multiple objectives. One way is to create one objective function, which contains various objectives (cost, total mass, etc.) where weighting can be assigned to one/some of the criteria in order to rank them against each other. An example of an optimization problem with two objectives, surface area A_s, and volume V, with weighting w_1 and w_2 could be;

$$min(f(A_s, V) = w_1 A_s + w_2 V) \tag{3.2}$$

or

$$min(f(A_s, V) = w_1 A_s / w_2 V) \tag{3.3}$$

The problem stated above gives two different results depending on how the objective function is written. Minimizing the top expression would minimize both the surface area and volume, while minimizing the bottom expression would minimize the area and maximize the volume.

Another alternative for multi-objective optimization is to explore the Pareto front. It is a visual approach to assess the trade-offs between the often competing objectives where the solutions are ranked by their level of domination rather than their performance in the objective functions.

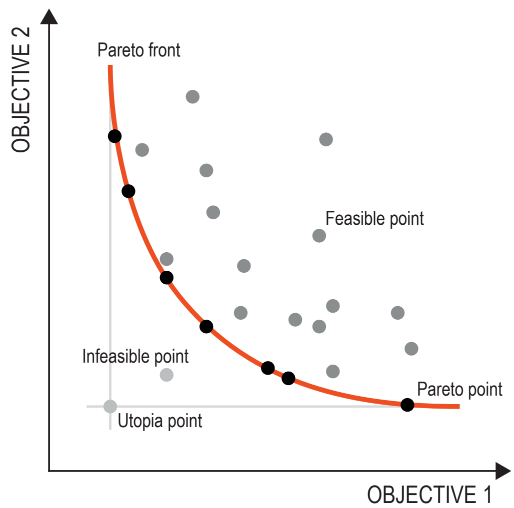

Figure 3.8 Pareto front for a bi-objective optimization problem.

By plotting the usually large number of evaluated solutions, an outer line can be identified which will define a border limit where the design solutions can't further improve. This limit is called the Pareto front which separates the feasible and infeasible regions, see Figure 3.8. This border will be a curve for a bi-objective problem, and a surface for a tri-objective problem. It is more complicated to visualize the Pareto front for a problem with more than three objectives. The points on the Pareto front are all possible optimal combinations of the objectives. For a point to be Pareto optimal, no objective can be improved without degrading at least one of the other objective values (Filomeno Coelho, et al., 2014).

There are usually multiple Pareto optimal solutions, making the solving of multi-objective optimization problems complex and not as straightforward as conventional single-objective optimization problems. The decision maker will need to choose from all of the multiple possible solutions, making this step very important. An experienced decision maker is therefore preferred, and the Pareto front could be used as a way of visualizing the different solutions, with the trade-offs between the different criteria.

3.2.2 Genetic algorithms

Genetic algorithms (GA) in optimization are a type of evolutionary algorithms inspired by the Darwinian law of natural selection. A random population of potential solutions is created from which the best individuals are favoured and combined in order to create better individuals at the next generation. The optimization process mimics the natural one for genetic mutation, reproduction and selection to iteratively improve the individuals in each generation, according to the optimization criteria (Richardson, et al., 2014). The GA process is stopped when a termination criterion has been met. The criterion can be related to the fitness function such that a minimum required fitness value has been reached, or it can be related to the number of solutions controlled, generations or the calculation time. For each generation, it is tested if the termination criterion is met and if it isn't, one more iteration will be performed.

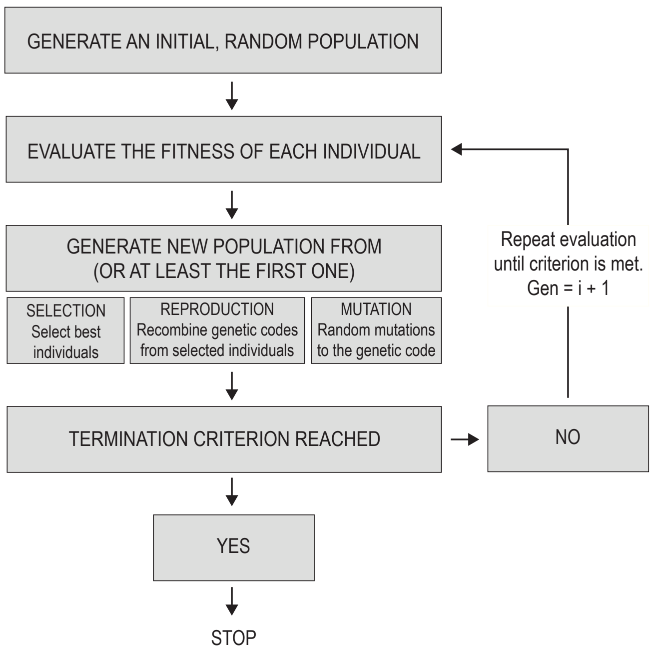

Figure 3.9 Flow chart of genetic algorithm optimization.

In multi-objective genetic algorithms (MOGA), diversity becomes an important aspect in the selection of individuals. The diversity operator controls how similar the design is compared to the rest of the population, which if promoted, leads to better exploration of the possible design solutions.

A risk related to the use of GA's is that the use of for example mutation and crossover can miss out on some possible solutions if the "wrong" parents are chosen. Some possible solutions that might result in more optimum solutions might be missed if for example the mutation rate is set too high. The calculation time for genetic algorithms are also higher compared to other optimization techniques. Genetic algorithms are however a good technique to search a large design space of complex problems, where the designer is not forced to pick a single optimal design but to choose from a final optimized population. Since the algorithm is random-search oriented, it does not rely on the initial point of search to be good, and can thus find optimal solutions for any starting point.

3.2.3 Generative design tools

Rhinoceros® is a computer-aided design tool developed by Robert McNeel & Associates. There are many possible plugins one can integrate in Rhino, one example is **Grasshopper®**. It is a visual programming tool that enables a parametric design process that immediately shows the progress and result in Rhino. Grasshopper consist of a set of components, that each contain several programming commands, that can be connected to each other on a canvas. The program enables parametric programming without the need of extensive scripting knowledge. Grasshopper is a free software and a lot of add-ons have been developed to broaden the use of the parametric modelling.

One of these add-ons is **Octopus**, an evolutionary optimization tool that can search for many objectives simultaneously. The component is connected to genes that will be changed during the optimization process, and objectives that are being minimized. It is also possible to connect hard constraints that have to be fulfilled for the solution to be kept in the generation. The program creates a Pareto front for each generation that enables the user to make trade-offs between the objectives. It enables one to choose preferred solutions during a search, promoting solutions similar to this. Octopus also allows the user to set generation size, number of generations, elitism (promotes local optimization mixing elite solutions), mutation probability, mutation rate, crossover rate and to promote genetical diversity.

The add-on **Kangaroo** is a physics engine that can simulate and calculate physical behaviour to enable interactive simulation, optimization and form finding. A solver weights different goals against each other in an iterative process until the nodes in the structure reaches equilibrium or a minimum energy threshold. As described in an earlier chapter, it can also be used to give a model a pseudo-physical behaviour, for example forcing faces on a mesh to be planar. This is useful working with geometries whose individual faces have more vertices than three.

Karamba is an add-on to Grasshopper that enables FE analysis in real time. Since it is implemented in Grasshopper it is possible to use together with for example Octopus and therefore enabling structural optimization. It is however more simple than many other FE-modelling programs, only performing linear analyses, which for the following study is considered to be sufficient.

3.3 Simple case study – 2D truss

In order to test the tools described above, a case study of a simple 2D truss has been performed. A truss is a suitable example for a first investigation, since the results can be predicted beforehand and understood and evaluated thereafter. Starting from the truss shown below, different input values will be changed according to selected objectives to reach optimal solutions. The optimization objectives will be:

- Maximize normal force utilization
- Minimize total mass
- Minimize deformations

The truss is loaded with self-weight and point loads at the top nodes. All connections are hinged and the bar elements all have the same circular tube cross section.

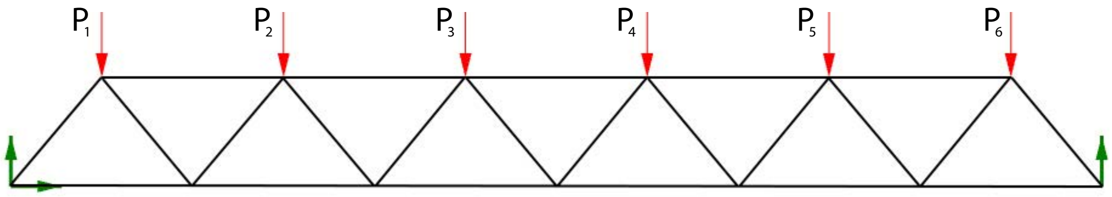

Figure 3.10 Initial truss.

Fixed variables:

$L = 10\ m$	Total truss span width
$\sum P_i = 50\ kN$	Sum of all point loads, all equal magnitude

Optimization variables:

$0.50\ m \leq h \leq 2.00\ m$	Truss height
$5.0\ cm \leq d \leq 15.0\ cm$	Cross section diameter
$0.20\ cm \leq t \leq 1.50\ cm$	Cross section thickness
$2 \leq n \leq 18$	Number of diagonals (even numbers)

Constrains:

$U_{N,i} = \frac{N_{Ed,i}}{N_{Rd,i}} \leq 1$	Normal force utilization limit
$l_i \leq 3\ m$	Bar length limit

Optimization objectives:

$max\left(\frac{\sum U_{N,i}}{2n-1}\right)$	Maximize sum of utilizations divided by number of bars
$min(\sum M_i)$	Minimize total mass
$min(max\lvert\delta_z\rvert)$	Minimize maximum deformation

Table 3.1 Variables and objective values for the initial truss.

	Height [m]	Diameter [m]	Thickness [m]	No. of diagonals	Average utilization [%]	Mass [kg]	Deflection [m]
Initial truss	1.00	0.100	0.0100	12	5	753.6	0.003

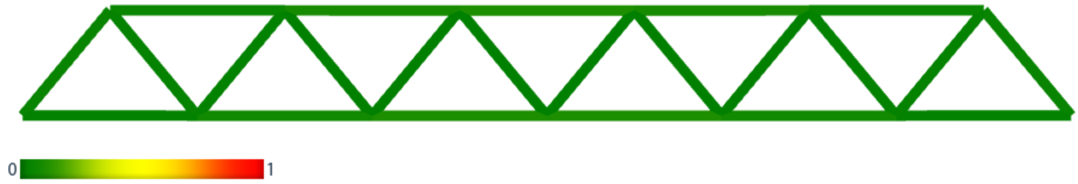

Figure 3.11 Initial normal force utilization.

After multi-objective optimizing with genetic algorithms trough Octopus, 100 generations with 100 individuals in each generation are produced. The results have different qualities since the objectives are conflicting. Three individuals from generation 1, 20 and 100 are shown on the next pages. They are chosen to represent three spread out results on the Pareto front from a 3D dimensional graph, see figure below.

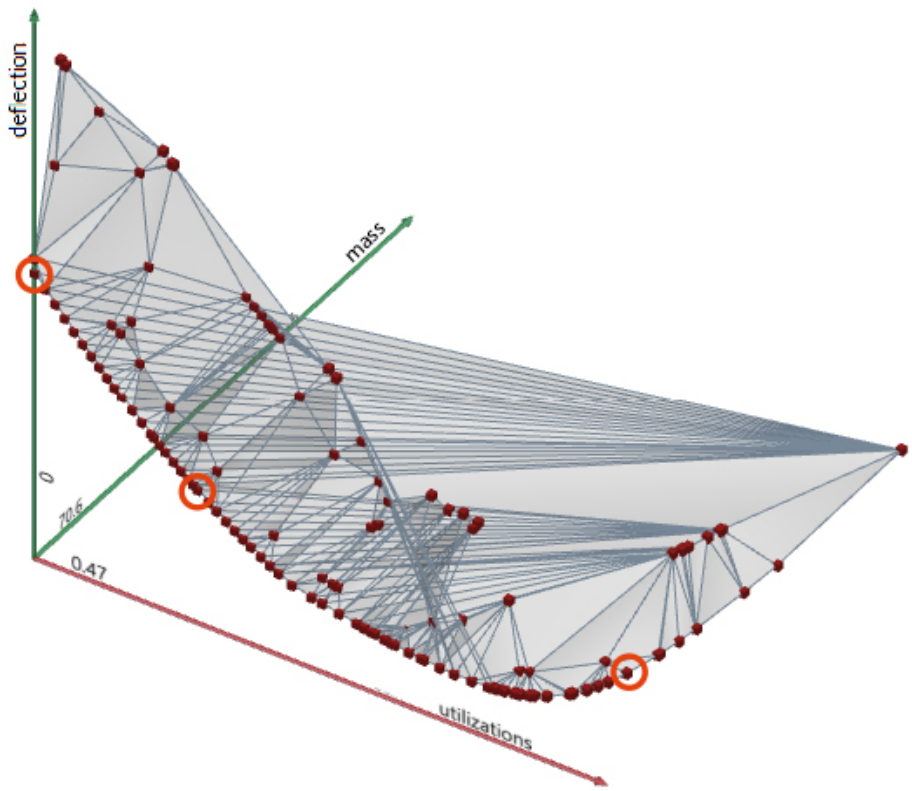

Figure 3.12 Three dimensional graph over the individuals on the Pareto front in generation 100.

Table 3.2 *Variables and objective values for the first generation.*

GEN 1	Height [m]	Diameter [m]	Thickness [m]	No. of diagonals	Average utilization [%]	Mass [kg]	Deflection [m]
Ind. 1	0.63	0.062	0.0038	12	29	168.4	0.025
Ind. 2	1.79	0.059	0.0032	8	16	154.0	0.005
Ind. 3	1.85	0.127	0.0038	10	6	450.6	0.002

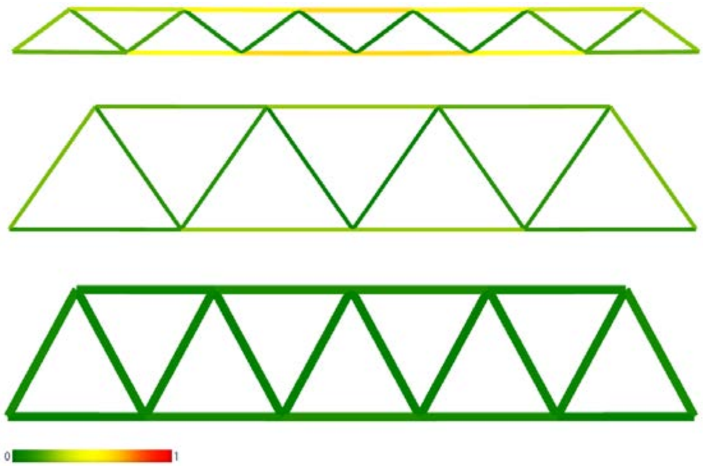

Figure 3.13 Individual 1, 2 and 3 generation 1, normal force utilization.

Table 3.3 Variables and objective values for generation 20

GEN 20	Height [m]	Diameter [m]	Thickness [m]	No. of diagonals	Average utilization [%]	Mass [kg]	Deflection [m]
Ind. 1	0.63	0.063	0.0025	8	47	107.0	0.039
Ind. 2	1.16	0.050	0.0021	10	39	82.0	0.018
Ind. 3	1.89	0.149	0.0029	16	6	528.7	0.002

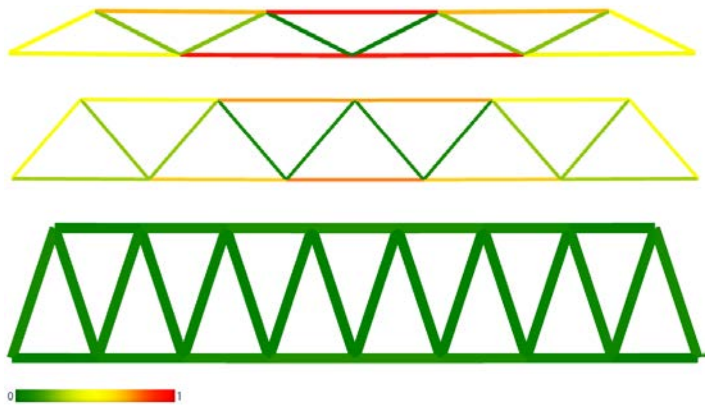

Figure 3.14 Individual 1, 2 and 3 generation 20, normal force utilization.

Table 3.4 Variables and objective values for generation 100

GEN 100	Height [m]	Diameter [m]	Thickness [m]	No. of diagonals	Average utilization [%]	Mass [kg]	Deflection [m]
Ind. 1	0.90	0.050	0.0020	8	53	70.6	0.031
Ind. 2	1.36	0.050	0.0020	8	37	76.4	0.015
Ind. 3	2.00	0.149	0.0026	8	7	341.4	0.002

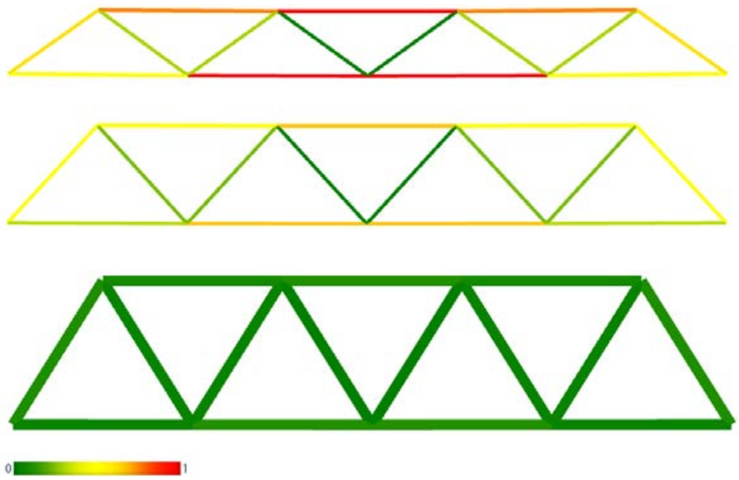

Figure 3.15 Individual 1, 2 and 3 generation 100, normal force utilization.

The result shows that the three individuals are well improved from the 1st to the 100th generation. The two first individuals have roughly the same mass, while the deflection and utilization is considerable different. The cross section diameter as well as the thickness is set to the lower limit value, making it clear that these values might need a second consideration. The third has very small deflections, but very low utilization and large mass.

4 Design project – implementation of theory

In this chapter, a study project will be designed in order to test and develop the method and theory described in previous chapters. The design project aims to follow the design process described in the figure below. The evaluation of the results can be just as important as the implementation of the design theory.

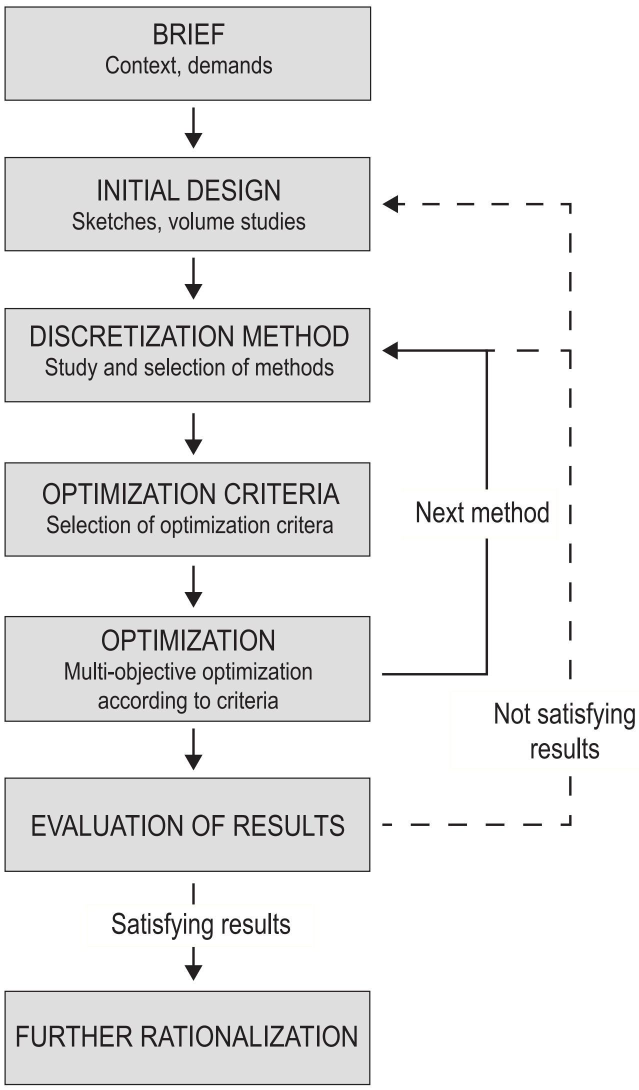

Figure 4.1 The design process chosen for this study project.

4.1 Brief

The design brief is to create a canopy, covering the courtyard of the civil engineering building at Chalmers University of Technology to provide rain and wind protection. It should cover parts of the courtyard, and still allow for sun light to reach into the surrounding buildings. The courtyard should have exterior climate, but the structure itself should be water tight. The façade facing south should be kept untouched to allow for a sunny seating area.

The structure is assumed to have simply supported conditions along the boundary of the courtyard, since there are columns and possibly floor slabs to connect to. The supports along the boundary is assumed to have fixed translational (x,y,z) and free rotational degrees of freedom.

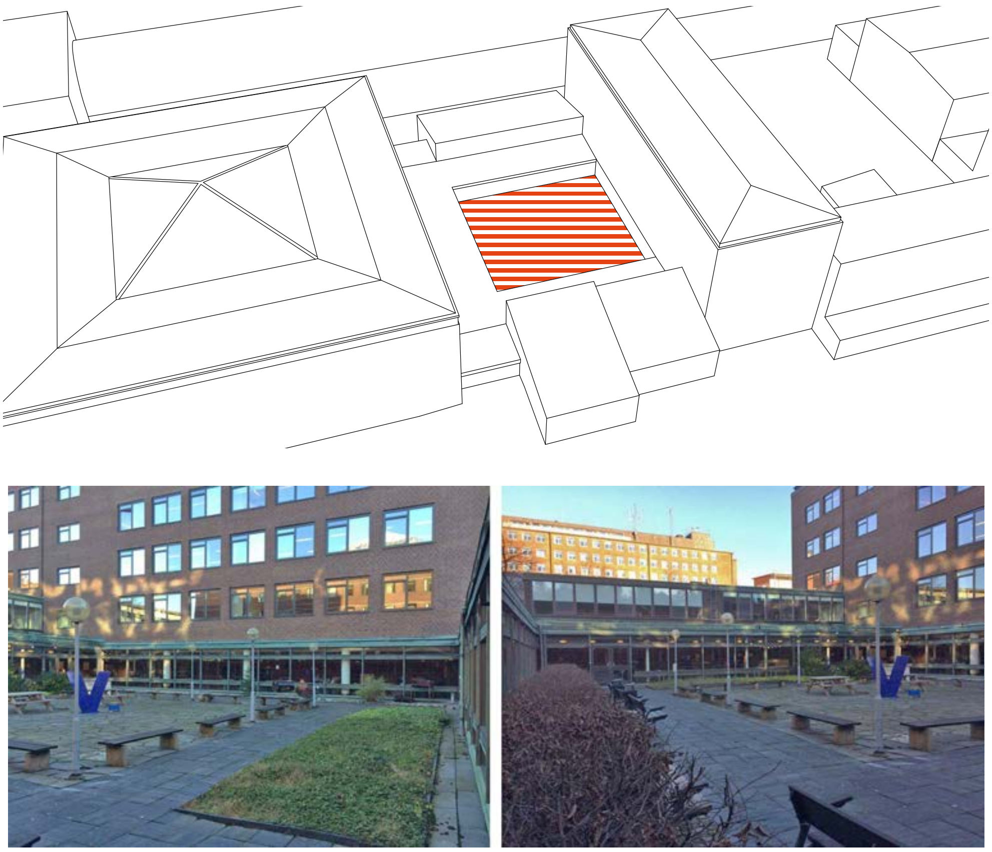

Figure 4.2 Existing courtyard at the civil engineering building, Chalmers University of Technology.

No dynamic or cyclic loads have been considered (vibrations, creep, shrinkage, etc.), neither has the detailing in connection between covering panels and grid structure. Geotechnical and foundation aspects have not been considered which can be an important factor for canopies in particular, where wind can cause the structure to lift. Therefore, the foundation and supports have to be able to withstand uplifting forces due to wind. The structural members is considered as round hollow steel cross sections.

4.2 Initial design surface

A set of initial designs were sketched and 3d-modelled where the aim was to create initial designs that differed from each other. Structural efficiency is considered to be one important factor for the final design. All initial designs have a curvature in order to more efficiently carry the loads.

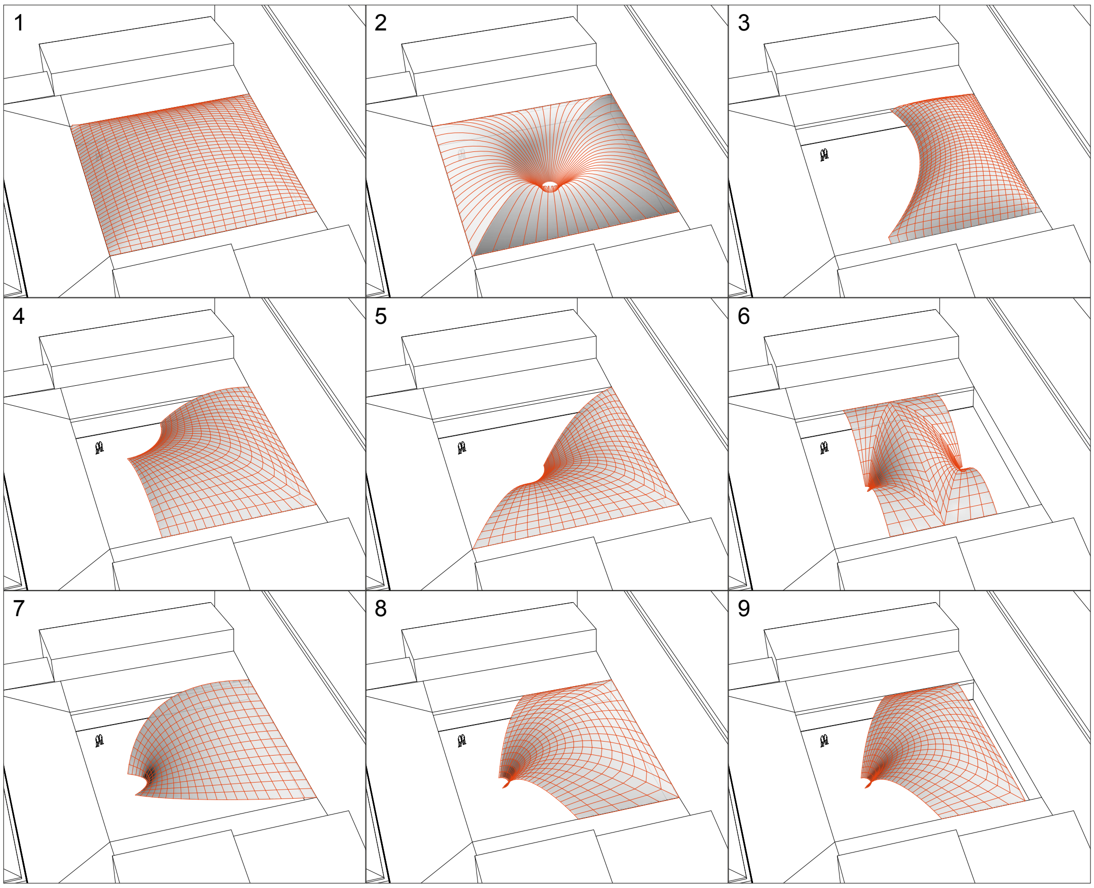

Figure 4.3 Initial designs of the roof covering the whole or parts of the yard.

The initial designs differ in covered area, curvature, structural boundary conditions and all-over shape. Design *1* and *2* are both covering the entire courtyard, and therefore neglected since they block the possibility for outdoor seating in the sun.

The remaining designs are similar, but design ***8*** in Figure 4.3 is chosen to be further developed. It creates a large covered area, where it is possible to pass the courtyard fully protected from rain (doors in each corner). It still leaves a big part uncovered in the area which will have most of the direct sun around noon.

The chosen shape will further be discretized and optimized according to certain criteria such as architectural aspects, structural efficiency and performance.

4.2.1 Loads

Loads acting on the structure has been calculated according to *Eurocode 2009*, see Appendix A for complete assumptions and calculations. Some geometric simplifications have been assumed, and the structure has been studied along the middle section shown in the sketches below.

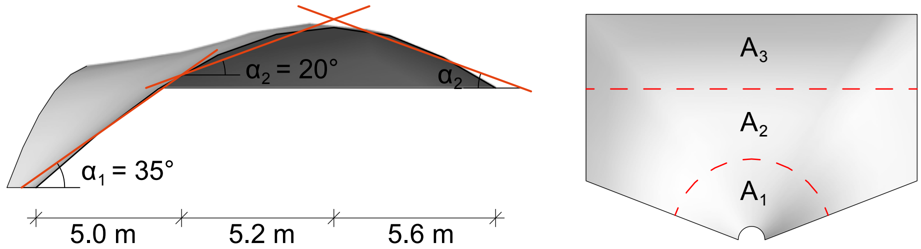

Figure 4.4 Geometric simplifications of the structure, showing the mid section (left) and top view (right). It is divided into three loading zones according to the slope of the canopy.

The calculated result is presented in each sub-chapter below.

4.2.1.1 Self-weight

The self-weight for the structural steel (S235) is calculated within the FE-program Karamba for every design as the geometry and dimensions change. The resulting load from the covering material is calculated in Appendix A. The total self-weight of the structure is calculated by:

$$G_{tot} = G_{steel} + G_{glass} \tag{4.1}$$

where

$G_{steel} = g\rho_{steel}V_{steel}$ Calculated within Karamba ($\rho_{steel} = 8\,000\ kg/m^3$)

$G_{glass} = g\rho_{glass}t_{glass}A_{glass}$ 6 mm glass panes ($\rho_{glass} = 2\,500\ kg/m^3$)

4.2.1.2 Wind load

The wind loads can be complex to calculate, especially for curved freeform surfaces. Simplified calculations with four load cases due to wind have been performed see Appendix A, but a wind tunnel test or computational study might have been required.

4.2.1.3 Snow load

The snow load is calculated according to load cases for a multi-span roof with a vertical wall on one side, see Appendix A. As for the wind, the shape of the canopy is simplified.

4.3 Application of surface discretization methods

Different meshes are applied to the surface to study suitable methods for sub-dividing the surface into smaller elements. For this surface, triangular and quadrilateral meshes are chosen to be studied more closely. These still provide large amount of solutions, from which only some have been developed. The figure below shows four different ways to triangulate the surface. All four meshes have planar faces since all faces are triangles. There are some advantages and drawbacks for the different meshes.

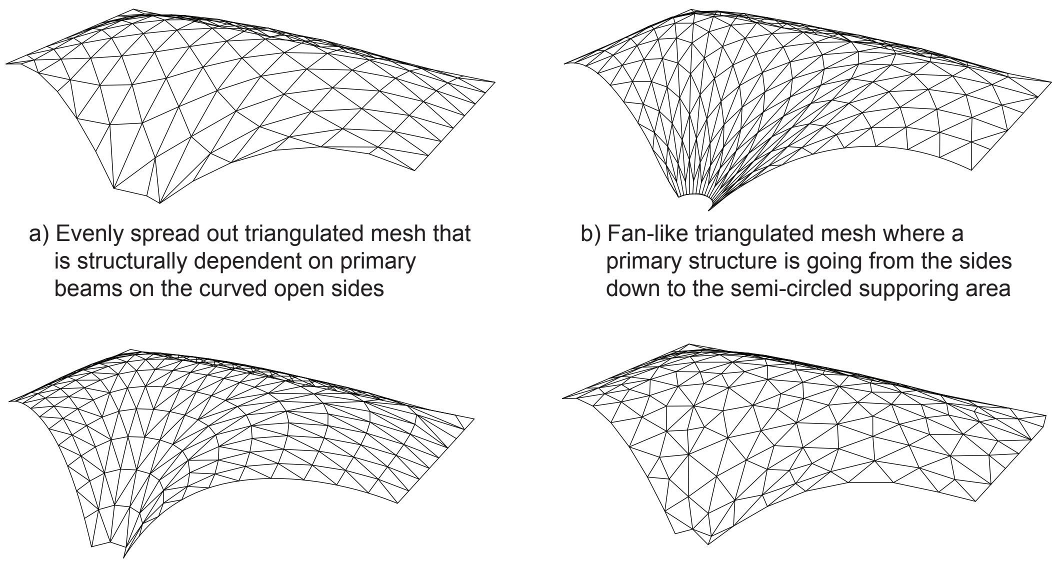

a) Evenly spread out triangulated mesh that is structurally dependent on primary beams on the curved open sides

b) Fan-like triangulated mesh where a primary structure is going from the sides down to the semi-circled supporing area

c) Triangulated mesh where the number of triangles is increased as the shape widens

d) Triangulated delaunay mesh created from randomly spread out points

Figure 4.5 Meshes with triangular faces.

Mesh *b* has a visual flow and may have some structural advantages since it has sets of bars going directly between the supporting boundaries and the ground. However, the space control is poor, meaning that the elements differ a lot in size. A way to avoid this could be to widen the semi-circle at the ground or to remove bars where the mesh is dense. Another way to achieve good spacing is to let the number of triangles increase as the shape widens, as in mesh *c*.

The Delaunay mesh, *d*, can seem irrational since it is created out of a random set of points, however, if these points are free to move during an optimization process, the structural members can be placed in optimal spots. This can on the other hand be hard to control, and it is also possible that a good optimal solution cannot be found. Both mesh *a* and mesh *d*, and somewhat *c*, have difficulties following the curvature at the semi-circled support, since the meshes have evenly spread out triangles.

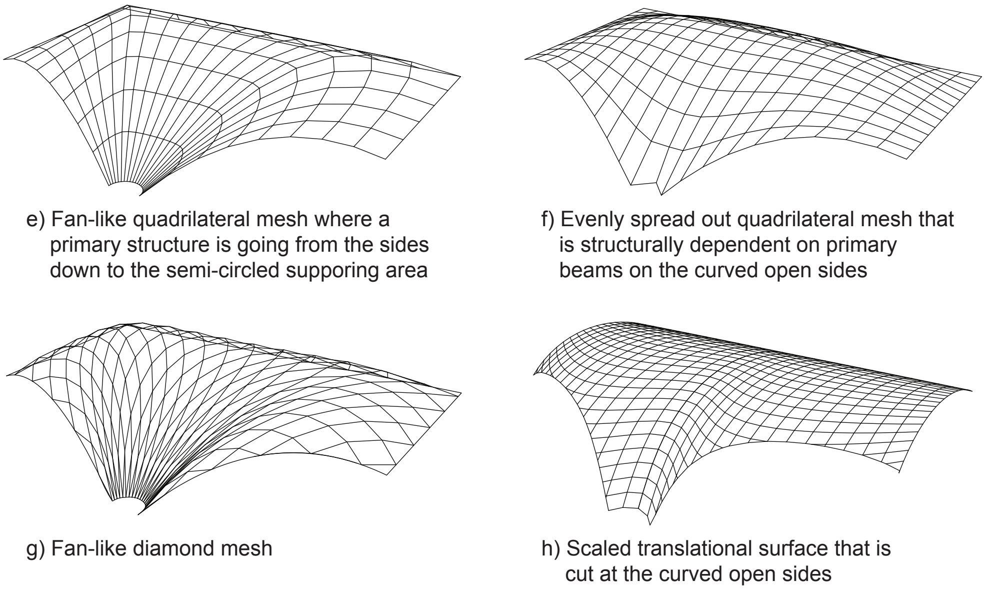

e) Fan-like quadrilateral mesh where a primary structure is going from the sides down to the semi-circled supporing area

f) Evenly spread out quadrilateral mesh that is structurally dependent on primary beams on the curved open sides

g) Fan-like diamond mesh

h) Scaled translational surface that is cut at the curved open sides

Figure 4.6 Meshes with quadrilateral faces.

Four different quadrilateral meshes are shown in the figure above. All meshes except h), the scaled translational surface, have double curved faces on this initial surface, no planarity optimization has been performed at this point.

Since the overall panel layout and shapes differ between these meshes, they have different potentials to have flat panels. Both mesh *e* and *g* have the same drawbacks as the triangulated mesh *b* with poor size control of the faces. Mesh *f* has the same problem as mesh *a* and *d* with difficulties following the curvature at the semi-circular support. For the scaled translational surface, *h*, all panels are flat due to its nature of being a bottom-up approach (see chapter 2, section 2.3.2.1). However, creating a surface like this has several limitations. The method is not always easy to control since the mesh layout is directly influencing the overall shape. It is therefore not suitable for all type of surfaces, and is thus not studied further.

After a planarity investigation, the meshes *f* and *g* have poor potential to have planar faces still keeping the desired shape. Since planarity of faces is seen as an important quality, these meshes are not considered in the next phase.

To limit the number of meshes to the optimization phase, meshes ***b***, ***c*** and ***e*** are chosen to be studied further.

4.4 Selection of optimization criteria

There are many, often conflicting, objectives to consider when designing a structure. These objectives contain both qualitative and quantitative aspects, which sometimes can be hard to evaluate. This is where the designer becomes an important factor of judging the result. To have a good overview of the optimization results, three different objectives are chosen. Other important criteria are set as hard constraints to ensure valid solutions.

In this study, the following have been considered:

Optimization objectives:

$min(m_{tot})$	Minimize total mass of the structure (steel and glass)
$min(\delta_{max})$	Minimize deformations under dead load
$min\left(\frac{A_{steel}}{A_{glass}}\right)$	Minimize the steel by glass area (maximize transparency)

Hard constraints:

Utilization for axial, bending and shear forces must not exceed 1 for any bar in the structure for all load cases. The Grasshopper FE-modelling add-on Karamba calculates these utilization rates, as well as combination of forces and moments, for the worst case for each structural member.

$$U_{N,i} = \frac{N_{Ed,i}}{N_{Rd,i}} \leq 1 \,, \qquad U_{M,i} = \frac{M_{Ed,i}}{M_{Rd,i}} \leq 1 \,, \qquad U_{V,i} = \frac{V_{Ed,i}}{V_{Rd,i}} \leq 1$$

Lengths of bars must not exceed 3.5 m for any bar in the structure:

$$L_i \leq 3.5\ m$$

Maximum deflection for any load case should not exceed:

$$\delta_{z,max} \leq \frac{L_{span}}{150} = \frac{15\ 000}{150} = 100\ mm$$

The deviation between vertices and a common plane (planarity) must not exceed:

$$\wp_i \leq 15\ mm$$

Optimization variables:

The following optimization variables and their limits are stated below:

d	Cross section diameter $50 \leq d \leq 200\ mm$
t	Cross section thickness $2.0 \leq t \leq 20.0\ mm$
n_x, n_y	Number of mesh divisions (x- and y-direction)
S_{load}	Inflation factor (to form find the surface)

4.5 Analysis & optimization of design alternatives

The three different mesh types are optimized according to the criteria listed above. Planarity is only studied for the quadrilateral mesh, since each triangular surface in a triangulated grid already has planar faces. The triangulated meshes is seen as a simply supported structure, with hinged joints between the bars, while the quadrilateral mesh is studied in two different cases, one case with fixed joints and one with hinged joints with diagonal bracing (see Figure 2.6). The edge beams at the open sides are considered as continuous beams.

The different meshes are generated for 100 generations with 100 individuals in each generation. The figure below shows the Pareto front of the last generation for the triangulated diamond grid. Four individuals from different zones on the front are displayed. The individual that is chosen closest to the origin, and is equally optimal for all three objectives, is considered as a good trade-off solution. One individual from this region is chosen for each of the meshes in the following chapters.

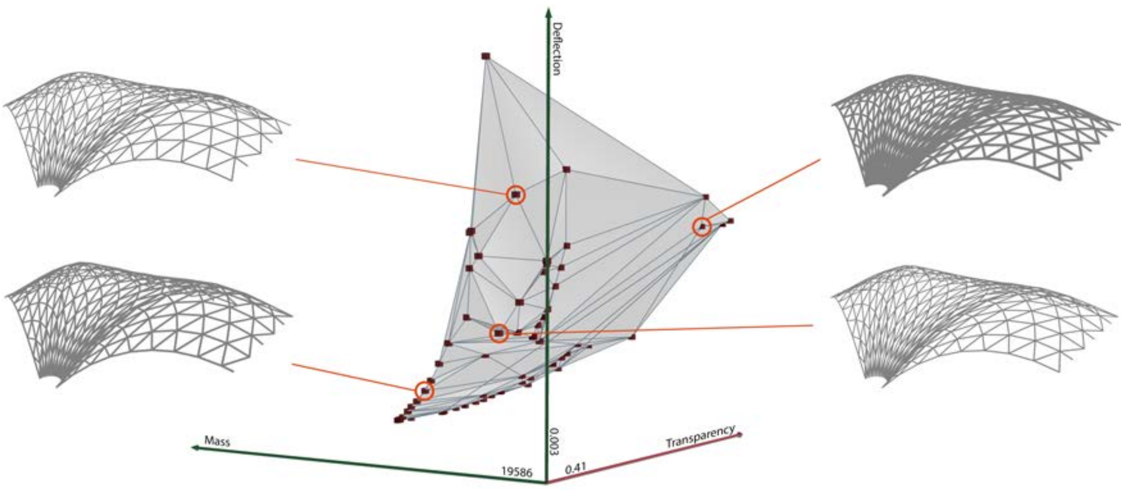

Figure 4.7 Three dimensional graph of the 100th generation of the triangulated diamond grid from Octopus, with four individuals on the Pareto front selected from different areas.

4.5.1 Triangular diamond grid

The result of the chosen individual is shown below in perspective and plan view. Since the structure has hinged connections, the members work mainly in tension and compression. The utilization graphs below shows the worst case for each bar. It shows that very few bars are highly utilized, while many of them have a low rate of utilization. This is because all bars have the same cross section, and this is something that should be studied further in a further rationalization phase.

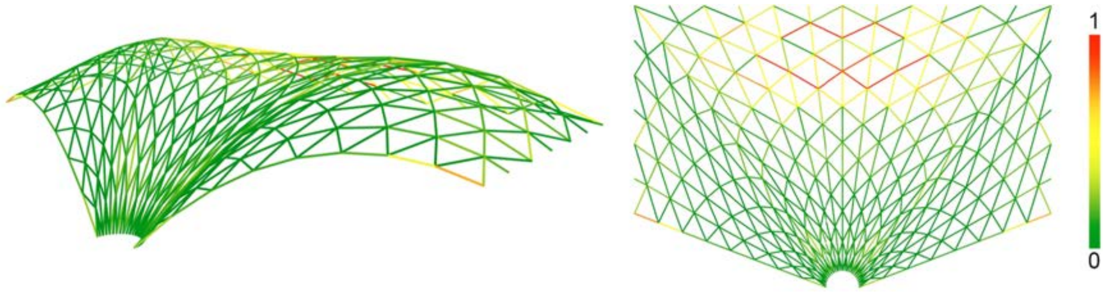

Figure 4.8 Pareto optimal individual. Utilization of the worst case for each bar.

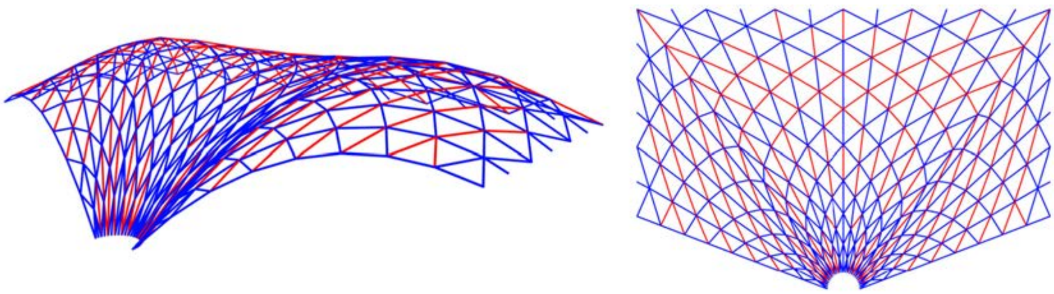

Figure 4.9 Tension (red) and compression (blue) under dead load.

The mesh layout enhances the shape as the lines flow between the supporting boundaries. The mesh layout and cross section thickness gives a good overall transparency of the grid, except for at the bottom part where the steel becomes very dense. This leads to big differences in the mesh element sizes, and the small angles between bars can lead to complicated nodes.

Table 4.1 Variables and objective values for the triangular diamond grid.

	d [cm]	t [cm]	δ_{max} [mm]	m [kg]	A_s/A_g [%]	U_{max} [%]
TRI DIAMOND	8.0	1.14	3.7	27 380	26	96

4.5.2 Branching grid

The following result shows the branching grid where the elements have similar sizes, unlike the previous triangulated diamond grid. Even though the utilization rate is more evenly spread out over the bars than for the previous mesh, the majority of the bars are still not very utilized. The bars are in this case hinged, making the members work mainly in tension and compression.

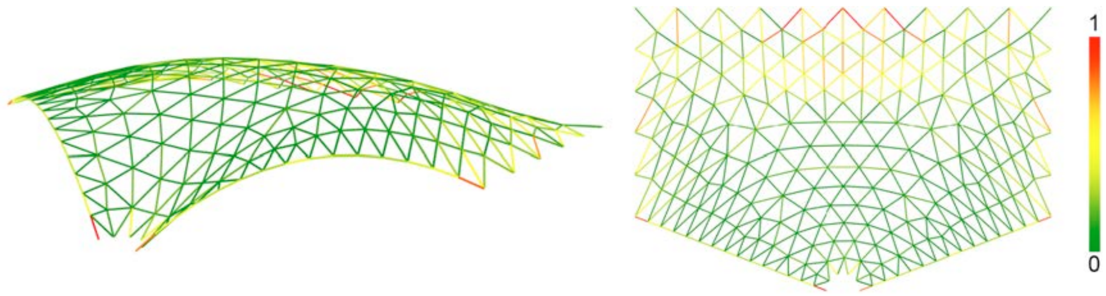

Figure 4.10 Pareto optimal individual. Utilization of the worst case for each bar.

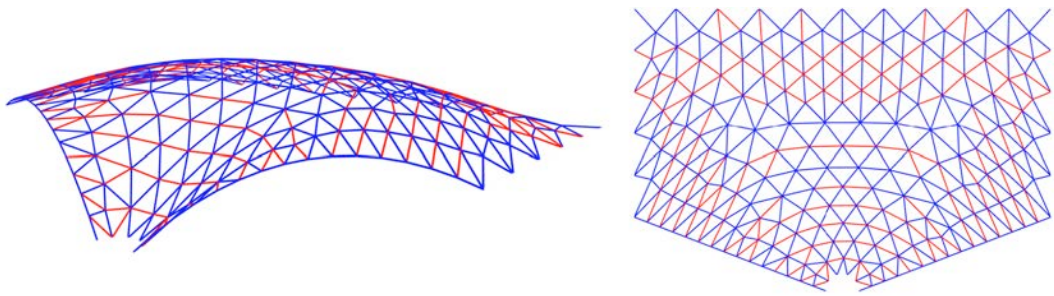

Figure 4.11 Tension (red) and compression (blue) under dead load.

Since the number of nodes increase as the shape widens, the size of the panels are more equal in size. However, odd valence nodes occur as a result of this. In those nodes, seven bars meet instead of six which is the case for the majority of the nodes. This results in a grid with disrupted lines, making the grid seem less continuously flowing. This is something that would need further refinement in a second design iteration in order to reach wanted aesthetic qualities.

Table 4.2 Variables and objective values for the triangular branched grid.

	d [cm]	t [cm]	δ_{max} [mm]	m [kg]	A_s/A_g [%]	U_{max} [%]
TRI BRANCH	7.0	0.80	9.5	17 857	20	99

4.5.3 Rectangular quadrilateral mesh - fixed connections

This is the only grid where all joints between bars are moment resistant connections. Because of this, the bars will not work mainly in tension or compression, but instead mainly in bending. The combination of moments and normal stresses are the critical case for the worst utilized bars, shown below. The utilization is evenly distributed for the rest of the bars, but still low degree of utilization.

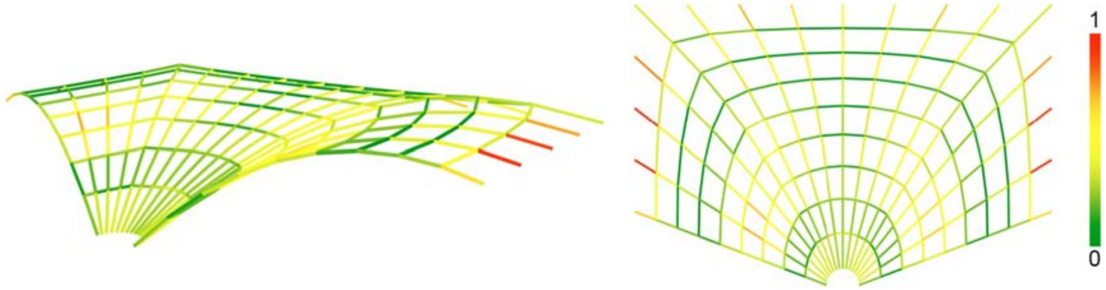

Figure 4.12 Pareto optimal individual. Utilization of the worst case for each bar.

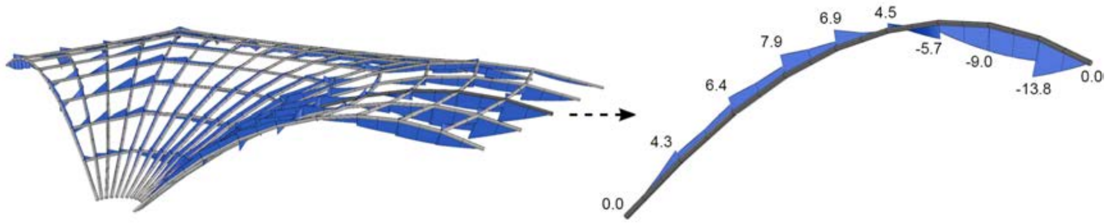

Figure 4.13 Bending moment (M_y) of the overall structure and the most utilized section [kNm].

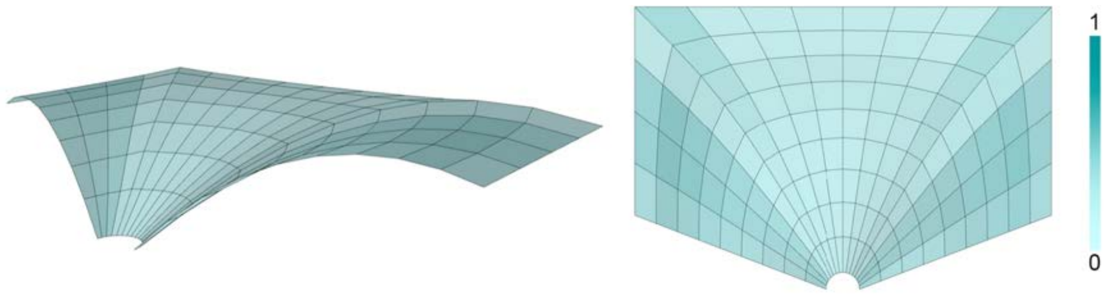

Figure 4.14 Planarity [cm]. Maximal deviation between vertices is 0.43 cm.

There is a large variation in panel size and shape for this grid. The planarity is sufficient according to the deviation tolerance, and satisfying in most areas. The global shape of the canopy is relatively low, a result of the planarity demand.

Table 4.3 Variables and objective values for the quadrilateral mesh with fixed joints.

	d [cm]	t [cm]	δ_{max} [mm]	m [kg]	A_s/A_g [%]	U_{max} [%]
QUAD FIXED	13.0	1.05	2.3	20 937	20	97

4.5.4 Rectangular quadrilateral mesh - diagonal bracing

This mesh is modelled as the previous one but with hinged connections and pre-stressed diagonal bracing (d_{cable}=2.6 cm) in each quadrangular. This way, the structure is still stable and all steel bars work mainly in compression. The utilization rate is evenly spread out, although no bar is fully utilized. In this case, the governing criterion is the deflections.

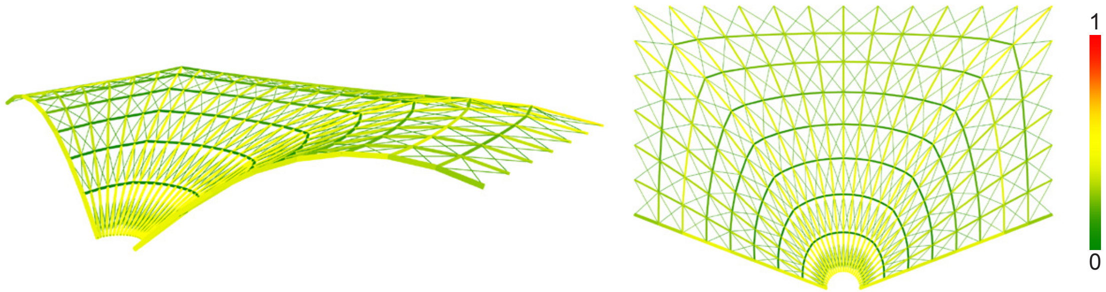

Figure 4.15 Pareto optimal individual. Utilization of the worst case for each bar.

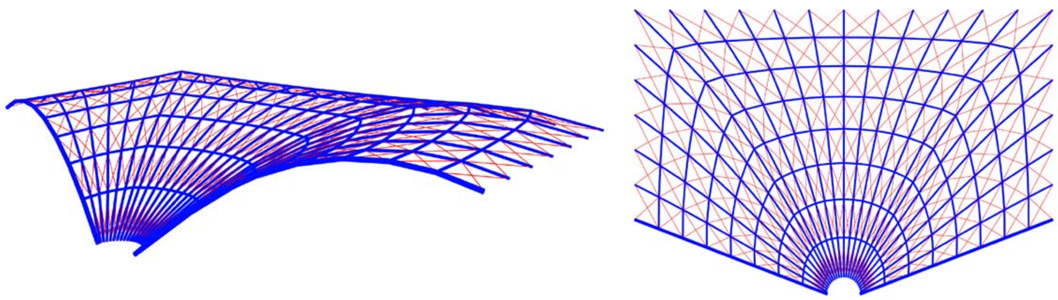

Figure 4.16 Tension (red) and compression (blue) under dead load.

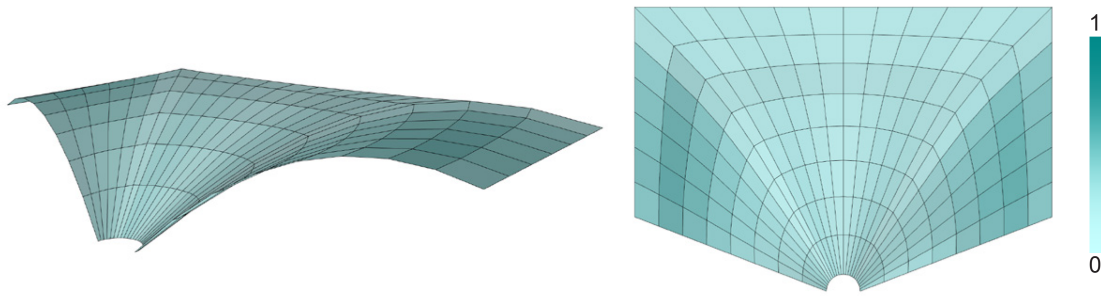

Figure 4.17 Planarity [cm]. Maximal deviation between vertices is 0.55 cm.

The mass is higher than for any of the other meshes. Since the structure is pre-stressed, the continuous beams at the open sides will receive higher stresses. This is compensated for by having a larger cross section at the side beams (d=19 cm, t=3.85 cm).

Table 4.4 Variables and objective values for the quadrilateral mesh with diagonal bracing.

	d [cm]	t [cm]	δ_{max} [mm]	m [kg]	A_s/A_g [%]	U_{max} [%]
QUAD DIAG	11.0	1.50	20.9	33 386	29	57

4.6 Evaluation and comparison of optimized meshes

The result from the optimization phase shows very promising results for all of the meshes. Different qualities and drawbacks are emphasised by each solution which will be presented in this chapter.

For both the quadrilateral grids and particularly the triangulated diamond grid, the steel grid is very dense at the grounds support. This could be improved either by enlarging the semi-circled support on the ground or by manually removing some of the bars. The triangulated grid would become a quadrilateral diamond grid at the bottom where the bars are removed. This would result in non-flat panels, which either could be solved by removing the glass panels or using curved glass in this particular area.

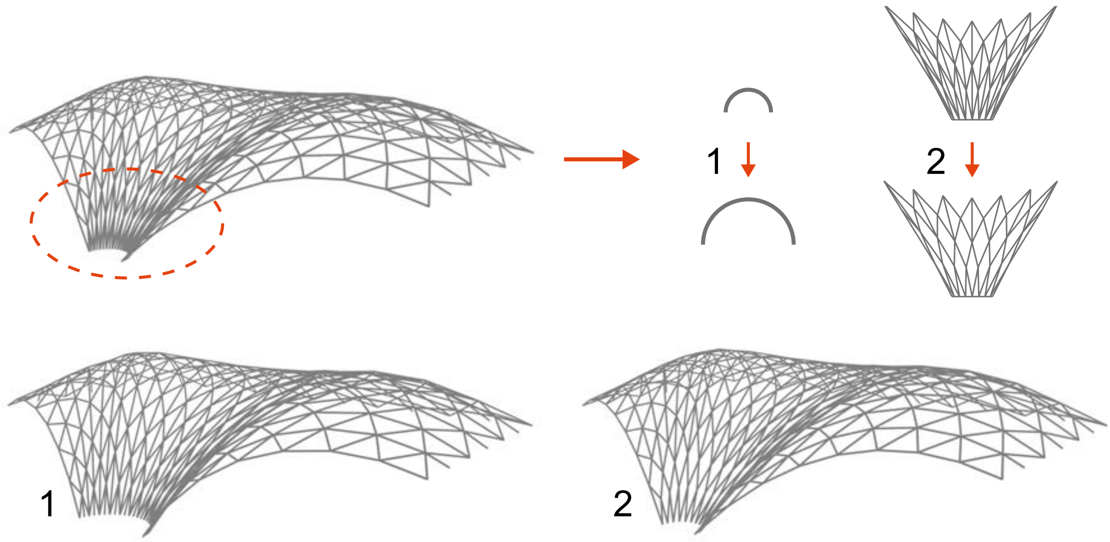

Figure 4.18 Illustrations of how the mesh layout and element size could be improved.

The branching grid is free from this issue since the mesh is defined such that the number of intersections between bars is increasing as the shape becomes wider. As mentioned earlier, odd valence nodes occur due to this, which disrupts the continuously flowing lines. This could be solved by either re-defining the way that more nodes are created, or by distributing the nodes in another way. One option could also be to return to the Delaunay mesh, where all points are more randomized. Disrupted lines would not be experienced as a problem since there are no continuous ones to begin with.

The first three of the previously studied meshes, triangulated diamond, branching and quadrilateral mesh with fixed joints, have a very low degree of utilization for most of the elements, and a few elements that approach 100% of utilization. This is a due to the fact that the same cross section is applied to all of the elements in the grid in this phase. The three meshes all have low deflections while the stresses reach the design value. However, the quadrilateral mesh with diagonal bracing is different where the large deflections are the governing criteria. Therefore, the utilization plot shows a more even distribution of the degree of utilization.

Both of the quadrilateral meshes are very low compared to the initial shape and the triangulated ones. This is a result of the planarization process. For the mesh with fixed joints, this is not a problem since it is capable of handling the stresses and deflection limits due to the overall rigidity of the structure. For the mesh with diagonal bracing however, the structure is more flexible and have larger deflections. A more curved shape would have helped in this aspect but it would be hard or even impossible to create flat panels.

The table below shows a summary of the selected individuals for each mesh. However, in order to fully compare the meshes to each other, more than one individual for each mesh would need to be presented.

Table 4.5 Variables and objectives for all meshes.

	d [cm]	t [cm]	δ_{max} [mm]	m [kg]	A_s/A_g [%]	U_{max} [%]
TRI DIAMOND	8.0	1.14	3.7	27 380	26	96
TRI BRANCH	7.0	0.80	9.5	17 857	20	99
QUAD FIXED	13.0	1.05	2.3	20 937	20	97
QUAD DIAG	11.0	1.50	20.9	33 386	29	57

As can be seen in the table above, the mass of the different grids varies between roughly 18 and 33 metric tons. This results in large difference in material usage and also how the structure affects the boundary supports.

The mass is somewhat related to the transparency (area of steel by area of glass), which varies from 20% to 29% for the studied individuals. It can be seen that the branched and the quadrilateral mesh with fixed nodes have the highest transparency. Quadrilateral meshes are often known to have good transparency, which is true in this case. It should be mentioned, however, that no extra steel has been added to compensate for the fixed nodes instead of hinged ones. Normally fixed nodes become a little bit larger and heavier than hinged ones since they need to be able to transfer moments.

The quadrilateral mesh with diagonal bracing has a low transparency, which is a result of the large cable dimensions and mesh density needed for the structure to fulfil the deflection limit. This could possibly have been solved by studying the pre-tensioning and cable quality in more detail.

4.6.1 Further rationalization

The following shows ways of how the grids can be further rationalized, including cross section optimization and reducing the number of unique panels. The triangulated diamond grid is presented below, in order to describe these processes. Further rationalization of the three other meshes can be seen in Appendix B and C.

4.6.1.1 Cross section optimization

To create an efficient structure, with well distributes stresses, the cross sections dimensions could vary. In order to reach a uniform structure, only the thickness of the cross section tubes are allowed to vary, and the diameter are kept the same. This will also reduce the self-weight of the structure, but might create a more complex and expensive manufacturing and construction phase. Therefore the number of different cross sections should be controlled. The figures below shows the utilization distribution and the cross section layout for 1, 2, 5 and 10 different number of cross sections. The diameters for all cross sections are the same, 80 mm, but the thickness vary between 3.0 and 20.0 mm.

In order to find a new cross section layout, the Karamba-component Optimize Cross Section is used. A set of pre-defined cross sections are chosen and distributed over the elements, keeping the stresses and deflections below the maximum values.

To be able to compare the mass of the construction material, the glass mass of 6 326 kg is removed from the total mass.

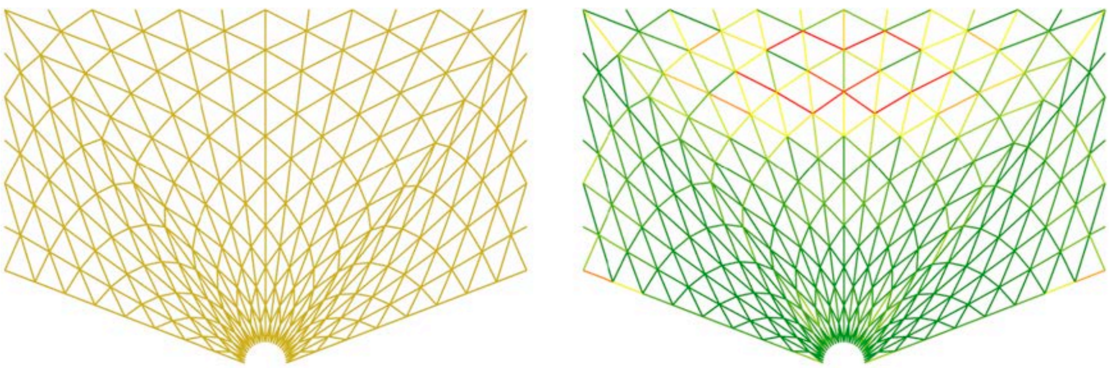

Figure 4.19 Initial cross section layout and utilization, m_{steel}=21 054 kg.

Table 4.6 Division and colour explanation of bars [mm].

Thickness	3.0	4.6	6.3	8.0	9.7	11.4	13.6	15.8	18.0	20.0
Colour										
No. of bars (1)	-	-	-	-	-	596	-	-	-	-
No. of bars (2)	-	464	-	-	-	132	-	-	-	-
No. of bars (5)	350	-	145	-	34	-	23	-	-	44
No. of bars (10)	324	92	55	34	13	10	11	12	4	41

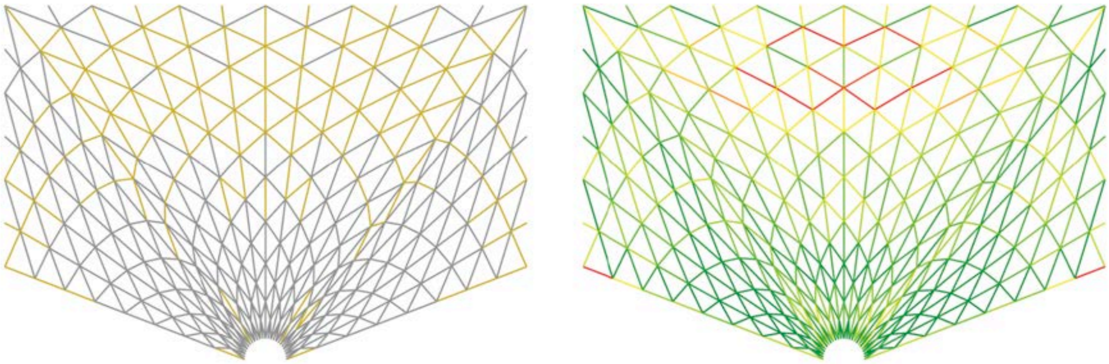

Figure 4.20 Cross section layout for 2 different types of bars and utilization, m_{steel}=13 145 kg. 38% mass reduction.

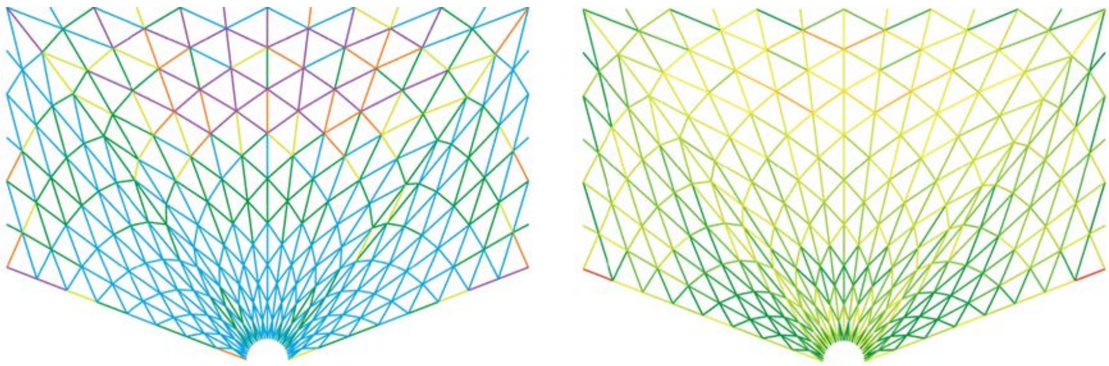

Figure 4.21 Cross section layout for 5 different types of bars and utilization, m_{steel} =11 450 kg. 46% mass reduction.

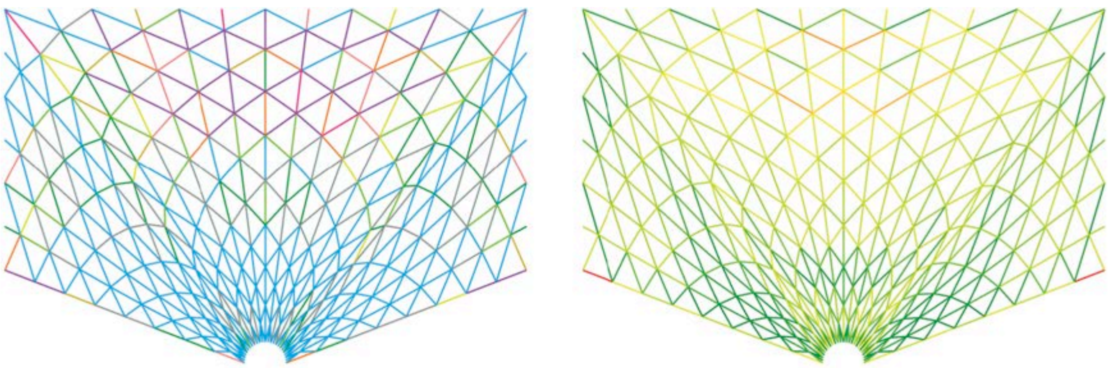

Figure 4.22 Cross section layout for 10 different types of bars and utilization, m_{steel} =11 422 kg. 46% mass reduction.

As can be seen in the figures above, the structure is able to have thinner bars in the earlier not fully utilized parts. With more than one different bar size, the mass can be reduced significantly. It can be seen that the largest reduction of the mass is between one and two cross sections. It can also be seen that there is almost no difference in mass between 5 and 10 different cross sections, which concludes that a relatively low number of different cross sections, that is higher than one, is a good solution for this structure.

In Appendix B, cross section optimization can be seen for the other grid designs, where for only a few different thicknesses of the bars, the mass can be considerably reduced for the other meshes as well. The triangulated branching grid and the quadrilateral grid with fixed joints has the largest difference in mass going from 1 to 5 different cross sections.

4.6.1.2 Reducing number of unique panels

As has been mentioned earlier in the theory chapter in the report, the number of different panels and nodes has an impact of the rationalization of the production phase. Depending on if the shape has symmetries or not, copies or mirrored copies of an element can be created naturally. In this case the shape is symmetrical along one axis, and therefore half of the elements will be mirrored copies of another. An additional way to make even more similar elements is to work with tolerances. If several elements are almost alike over the mesh, the total number of different elements can be lowered.

SmartClustering is a Grasshopper add-on created by the SMART Solutions Network at Buro Happold Engineering. It is used for reducing the number of unique panels of a surface. The algorithm is based on a variation of the K-means algorithm, which sorts the panels by their sizes and shape, and groups the ones that are similar to each other. The panels in the group is then replaced by a master panel, which represents an average of the panels in the group (Sharma, 2015). The component allows for the user to specify either the number of wanted unique panels, or the tolerance of the maximum deviation from the initial surface.

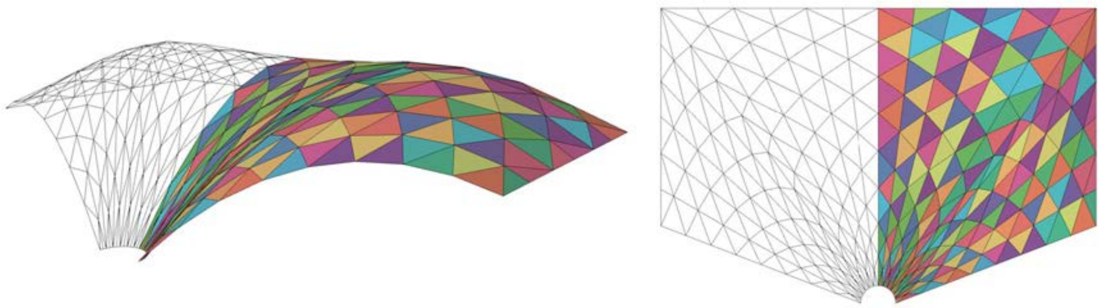

Figure 4.23 Initial face layout. All 204 panels are unique.

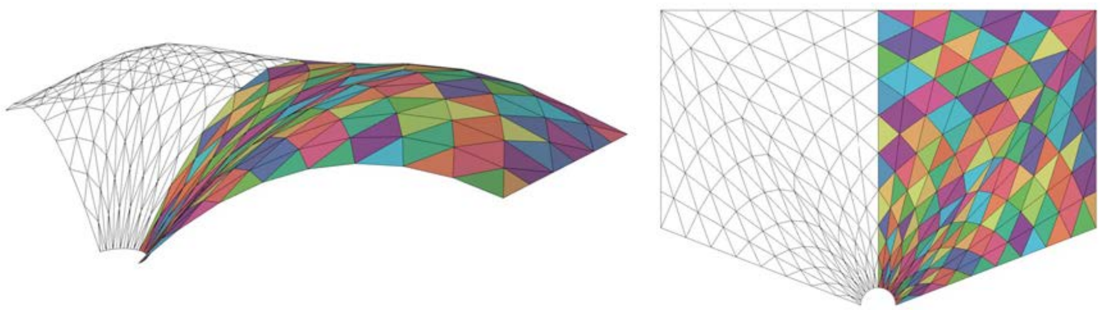

Figure 4.24 168 unique panels. Deviation = 0.01 m. 18% reduction.

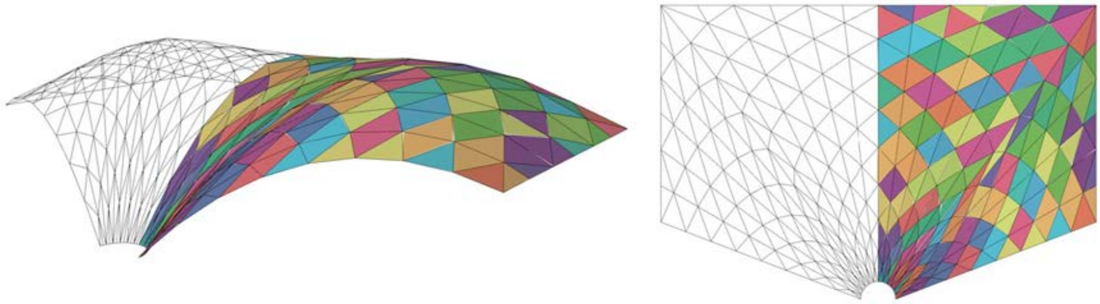

Figure 4.25 80 unique panels. Deviation = 0.105 m. 61% reduction.

The component is used for the triangulated diamond mesh above and the other meshes can be found in Appendix C. The figures above shows the initial mesh and the mesh clustered with 168 respectively 80 unique panels. Due to symmetry, only half of the mesh is studied where the different faces are illustrated with different colours.

Figure 4.26 *Deviation between panels. From the left: Clustering of 204, 168 and 80 unique panels.*

With the tolerance of 0.01 m, 168 unique panels can be used instead of 204. This is a reduction of approximately 18%. This reduction can seem small, but for a larger projects this could become a big cost saving technique.

In Appendix C, it can be seen that the reduction of number of unique elements is best for the meshes with triangular faces. Since the number of panels are much higher to begin with, it is also easier to find a higher percentage of similar elements. Since the triangular diamond grid has triangles created out of quadrilateral diamonds, where each pair are relatively similar, it is promising to cluster this mesh. However, since the quadrilateral meshes have fewer panels to begin with, the gains of creating duplicates are not as big.

Depending on the type of panel, the advantages of reducing the number of unique elements vary. In this study project, it is not of a very high importance, since the production of flat single layer glass panels is simple. If they were more complex, or if the panel would for example require a mould (because of e.g. double curvature), great gains could be made. Then the mesh should initially have been adapted according to this.

5 Discussion

5.1 Conclusion and discussion

As shown in this thesis, the rationalization process can be very complex and difficult with many different aspects to consider. This thesis work is focused on discretizing freeform surfaces and therefore, other ways of rationalizing these shapes will not be discussed. The design project shows that the discretization methods have different advantages and drawbacks depending on the specific case. A large part of the rationalization process is understanding and implementing different constrains early on. Examples of this could be finding a form that has the potential of being structurally optimized, to develop a suitable mesh with rational layout or panels and nodes that can be produced in a feasible and affordable way. One other important aspect can be to allow the initial shape to change according to the constrains and objectives.

Even though limitations in terms of constructability etc. are a big part of rationalization, they should not be seen only as something negative. They can also be very inspiring. However, it is important to always question the limitations and try to challenge and develop them. If not, architecture and structural design might never evolve. This is where the designer plays an important role of understanding the limitations in order to make use of them in the best way.

If freeform shapes are defined to be smoothly flowing shapes without symmetries and structural logic, it could be questioned whether it’s possible to rationalize them at all. Is a rationalized freeform surface still a freeform surface? From an economical and sustainable point of view, it is our belief that all projects should go through some rationalization.

5.1.1 Design approaches

When the two design approaches top-down and bottom-up were presented in the report, it was mentioned that a combination of the two probably is a good way of reaching a good and rational design process and result. With a bottom-up approach, the designer can make sure that the project is buildable but it also requires more knowledge from the start of the project. Combining this with a top-down approach, the overall design will still be kept making sure that the initial intention is not sacrificed too much.

Form finding is typically categorized as a top-down approach, while pre-determining maximum element size or planarity constrains can be examples of bottom-up approaches. When iterating numerous solutions over many generations, in a multi-objective search with several constraints in a parametric environment, the two approaches are combined. The exact shape and mesh layout of the surface is developed according to a combination of structural and aesthetical constraints. In a further development of the design, more constraints and objectives could be added. As an example, the cross sections could be more adapted to what is available on the market.

5.1.2 Optimization

It has been mentioned in the theory of genetic algorithms that they can be very useful when searching for solutions to complex problems, but that they do not guarantee that an optimal solution is reached. In the study project of the steel and glass canopy, it can be seen that the designs are improved over the generations with respect to the objectives. The selected solutions of the 100th generations were much better than the result of initial manual testing of different variables beforehand, showing that the optimization process enhanced the use of parametric design by broad testing and development. The resulting Pareto front gives a perspicuous representation of the best individuals and makes it easy for the designer to understand the trade-offs between the different objectives to make informed decisions.

A few different combinations of mutation rate, crossover rate and elitism, were studied for one of the meshes. The different combinations gave similar results, and therefore one of the combinations was used for all of the other meshes. It should also be noted that the different rates were the same over all generations. Gains could have been made if these were changed in the process. For example, the diversity could be best kept high in the beginning to of the search along with the crossover rate, to explore many possible solutions, and smaller at the end, when hopefully all local optimum were found.

A convergence study should have been performed in order to ensure that the optimization process had reached a final solution. In the study project, the generations was pre-decided to 100, and it was therefore not guaranteed that the optimization had reached convergence. In order to control this, it was verified that the difference between the previous generations were small.

Since both the clustering and cross section optimization was applied as a further rationalization step after the multi-objective optimization phase, they had no way of influencing the resulting shape of the design surface. This was due to the fact that both of the components are computational expensive, making the multi-objective optimization process very time consuming. However, it would have been interesting to study how the resulting surface would have turned out if this was implemented.

In this study, details of the connections between bars and the attachment of the glass panels were not studied. This could have led to more refined constraints in the optimization and could have given limitation to the grids.

As a conclusion, the thesis shows that the use of genetic algorithms and parametric design can be very effective for generating many different solutions to complex freeform architectural problems. However, the role of the designer is still very important when it comes to judging the result and selecting a design based on qualitative objectives.

5.1.3 Constructability

One of the focus points of the design project has been to create a freeform surface with flat panels. This is due to the increase of cost at the production stage, for how curved panels is produced today. Flat panels are much cheaper to manufacture than both single and double curved ones. This is especially true when it comes to glass, which was the cladding material chosen in the design project. However, digital design and the production methods are evolving and with future techniques the difference in cost between curved or flat glass might decrease. Nevertheless, depending on the curvature, it may not be structurally efficient for the separate elements to be curved, therefore there could still be of importance to create flat panels.

The process of reducing the number of unique elements, shows a quite small reduction for the study project with the specified tolerance of 0.01 m, it can be of more importance for larger projects. If for example the British museum mentioned above would have had a similar result, the number of unique panels could have been reduced from 3312 to 2716. However, depending on the production technologies, this issue might not be of high importance. Techniques such as CNC milling or similar can create many different shaped flat panels relatively easy. In the near future additive manufacturing, often known as 3d-printing, of optically transparent glass can become available for the building industry making curved panels with different shapes cheaper than today.

In the study project, only the panels have been studied in a further rationalization process in order to reduce the number of unique ones. Instead, it might have been of interest to study the number of different nodes as they often are more complex and expensive to produce. Although, these may be even easier to produce by 3d-printing technique in the near future.

5.2 Future work

As a continued study, a second iteration could have been performed for all meshes according to the comments at the evaluation. The conceptual designs could be developed further regarding a more thorough analysis with detail design and checking reaction forces against support conditions. More detailed load conditions would also have been necessary if the structure were to be built. In a freeform shape study like this, other architectural and engineering aspect such as acoustics or heat caused by solar radiation could have been taken into consideration as objectives in the optimization phase, and the result could have been very different.

Both the reduction of unique panels and cross section optimization are applied at the end of the design process, similar to the top-down approach. Further development of this thesis could be to analyse how the result would change if the different objectives in the optimization process were applied in another order. The form finding could take place outside of the optimization engine Octopus, and instead clustering and/or cross section optimization could be included and so on. A rationalization study where the intersections between elements were studied more closely would also have been interesting, as that is something which has impact on the simplicity in design and constructability.

6 References

Davidsson, U., 2015. *Meeting about Emporia Shopping Centre* [Interview] (2 October 2015).

Eden Project, 2001. *Architecture at Eden.* [Online]
Available at: https://www.edenproject.com/eden-story/behind-the-scenes/architecture-at-eden
[Accessed 12 October 2015].

Eigensatz, M. et al., 2010. Paneling Architectural Freeform Surfaces. *ACM TOG - Proceedings of ACM SIGGRAPH,* 29(4), p. Article No. 45.

European Committee for Standardization, 2009. *Eurocode - Basis of structural design (Eurocode SS-EN 1990).* Stockholm: SIS Förlag AB.

European Committee for Standardization, 2009. *Eurocode 1: Actions on structures - Part 1:1 General actions - Densities, self-weight, imposed loads for buildings (Eurocode SS-EN 1991-1-1).* Stockholm: SIS Förlag AB.

European Committee for Standardization, 2009. *Eurocode 1: Actions on structures - Part 1-3: General actions - Snow loads (Eurocode SS-EN 1991-1-3).* Stockholm: SIS Förlag AB.

European Committee for Standardization, 2009. *Eurocode 1: Actions on structures - Part 1-4: General actions - Wind actions (Eurocode SS-EN 1991-1-4).* Stockholm: SIS Förlag AB.

Filomeno Coelho, R., Méndez Echenagucia, T., Pugnale, A. & Richardson, J. N., 2014. Genetic algorithms for structural design. In: S. Adriaenssens, P. Block, D. Veenendaal & C. Williams, eds. *Shell Structures in Architecture.* New York: Routledge, pp. 290-294.

Grange, K., 1998. *Kulturkrock eller Brobygge,* Master's thesis, Department of Architecture, Chalmers University of Technology, Göteborg.

Hesselgren, L., 2009. Generative Design - Changing the Face of Architecture. *Be Current,* 6(3), pp. 20-23.

Mitchell, W. J., Liggett, R. S. & Tan, M., 1988. *The Topdown system and its use in teaching.* [Online]
Available at: http://cumincad.architexturez.net/system/files/pdf/8403.content.pdf
[Accessed 10 November 2015].

Nero, I., 2004. *Computers, Cladding, and Curves: The techno-Morphism of Frank Gehry's Guggenheim Museum in Bilbao, Spain,* Tallahassee, Florida: Florida State University.

NEY+Partners, 2011. *Glazed roof, The National Maritime Museum, Amsterdam completed.* [Online]
Available at: http://ney.be/jp/news_details/135.html
[Accessed 07 October 2015].

Olsson, J., Tsigkari, M. & Aish, F., 2015. *Meeting about Mexico City Airport* [Interview] (6 November 2015).

Pottman, H., Brell-Cokcan, S. & Wallner, J., 2006. *Discrete Surfaces for Architectural Design.* Avignon, Nashboro Press, pp. 213-234.

Pottman, H. et al., 2008. Freeform surfaces from single curved panels. *ACM TOG - Proceedings of ACM SIGGRAPH*, 27(3), p. Article No. 76.

Pottmann, H., 2014. *Public Lecture: Mathematics in Modern Architecture.* [Online]
Available at: http://www.ima.umn.edu/videos/index.php?id=2653
[Accessed 07 10 2015].

Richardson, J. N., Adriaenssens, S., Filomeno Coelho, R. & Bouillard, P., 2014. Discrete Topology Optimization. In: S. Adriaenssens, P. Block, D. Veenendaal & C. Williams, eds. *Shell Structure in Architecture.* New York: Routledge, pp. 170-179.

Schlaich Bergermann Partner, 2005. *New trade fair in Milan: Logo & Vela.* [Online]
Available at: http://www.sbp.de/en/project/new-trade-fair-in-milan-logo-vela/
[Accessed 07 October 2015].

Schlaich, J. & Bergermann, R., 2005. *Light Structures.* 2nd ed. Munich: Prestel Verlag.

Schober, H., Glymph, J., Ceccato, C. & Mussel, J., 2002. *A Parametric Strategy for Freeform Glass Structures Using Quadrilateral Planar Facets.* Pomona, ACADIA, pp. 303-321.

Sehlström, A., 2013. *Multi-Objective Topology Optimization: Tracing of Pareto-optimal structures with respect to volume, compliance and fundamental eigenvalue,* Master's thesis 2013:18, Division of Applied Mechanics, Chalmers University of Technology, Göteborg.

Sharma, S. B., 2015. *SmartClustering.* [Online]
Available at: http://www.smart-solutions-network.com/page/smart-clustering
[Accessed 21 December 2015].

Wang, W. & Liu, Y., 2010. A Note on Planar Hexagonal Meshes. In: I. Z. Emiris, F. Sottile & T. Theobald, eds. *Nonlinear Computational Geometry.* New York: Springer, pp. 221-233.

Veenendaal, D. & Block, P., 2014. Comparison of form-finding methods. In: S. Adriaenssens, P. Block, D. Veenendaal & C. Williams, eds. *Shell structures in architecture.* New York: Routledge, pp. 115-129.

Williams, C. J. K. & Shepherd, P., 2010. British Museum Great Court. In: J. Burry & M. Burry, eds. *The New Mathematics of Architecture.* New York: Thames & Hudson, pp. 122-125.

Zadravec, M., Schiftner, A. & Wallner, J., 2010. *Designing Quad-dominant Meshes with Planar Faces.* Oxford, Blackwell Publishing, pp. 1671-1679.

6.1 Figure references

If other not expressed below, the rights of the pictures and illustrations in the report belong to the authors.

Figure 1.1 Left: Expo 58 by Wouter Hagens (Own work)
[GFDL (http://www.gnu.org/copyleft/fdl.html) or CC BY-SA 3.0 (http://creativecommons.org/licenses/by-sa/3.0)], via Wikimedia Commons
URL: *https://upload.wikimedia.org/wikipedia/commons/e/e7/Expo58_ building _Philips.jpg*
[Accessed 4 October 2015]

Right: Sydney Opera House by Bjarte Sorensen. (Own work)
[GFDL (http://www.gnu.org/copyleft/fdl.html) or CC-BY-SA-3.0 (http://creativecommons.org/licenses/by-sa/3.0/)], via Wikimedia Commons
URL: *https://upload.wikimedia.org/wikipedia/commons/9/98/SydneyO peraHo use.jpg*
[Accessed 4 October 2015]

Figure 1.2 Left: Olymipastadion München by btr (Own work) *[CC BY-SA 2.5 (http://creativecommons.org/licenses/by-sa/2.5)], via Wikimedia Commons*
URL: *https://upload.wikimedia.org/wikipedia/commons/9/92/ Olympiastadion_M%C3%BCnchen_%281972%29_01_b.JPG*
[Accessed 18 December 2015]

Right: Hippo House, Berlin Zoo. ©Schlaich Bergermann und Partner
URL: *http://www.sbp.de/en/project/house-for-hippopotamus-zoo-berlin/*
[Accessed 4 October 2015]

Figure 1.3 New Trade Fair in Milan by ©Ramon Prat
URL: *http://www.fuksas.it/en/Projects/New-Milan-Trade-Fair-Milan*
[Accessed 10 December 2015]

Figure 2.4 Left: The Great Court. Public domain.
URL: *https://commons.wikimedia.org/wiki/File:The_Great_Court.jpg*
[Accessed 5 October 2015]

Figure 2.7 Basic principle for planar quadrilateral meshes. Courtesy of Hans Schober.
Schober, H., Glymph, J., Ceccato, C. & Mussel, J., 2002. *A Parametric Strategy for Freeform Glass Structures Using Quadrilateral Planar Facets*. Pomona, ACM, pp. 303-321.

Figure 2.9 Glass Roof of the Museum of Hamburg History by ©Heiner Leiska.

Figure 2.11 Left: Guggenheim Museum Bilbao. Public domain.
URL: *https://www.flickr.com/photos/boklm/12141898293/in/photolist-juWpm2-juWmER-yKpGuU-xQGgSu-xQGh1L-yMJ5Uz-yNuwWx/*
[Accessed 16 October 2015]

Right: Guggenheim Museum Bilbao. Public domain.
URL: *https://www.flickr.com/photos/76743870@N00/21494649716/in/photolist-juWpm2-juWmER-yKpGuU-xQGgSu-xQGh1L-yMJ5Uz-yNuwWx/*
[Accessed 16 October 2015]

Figure 2.13 Left: Hungerburgbahn-Bergstation by Hafelekar (Own work) *[CC BY-SA 3.0 (http://creativecommons.org/licenses/by-sa/3.0)], via Wikimedia Commons*
URL: *https://upload.wikimedia.org/wikipedia/commons/f/f6/Hungerburgbahn-Bergstation.JPG* [Accessed 7 October 2015]

Right: Graz Kunsthaus vom Schlossberg by Marion Schneider & Christoph Aistleitner *[CC BY-SA 2.5 (http://creativecommons.org/licenses/by-sa/2.5)], via Wikimedia Commons*
URL: *https://upload.wikimedia.org/wikipedia/commons/9/9b/Graz_Kunsthaus_vom_Schlossberg_20061126.jpg* [Accessed 7 October 2015]

Figure 2.16 Left: New Milan Trade Fair by ©Studio Fuksas
URL: *http://www.fuksas.it/en/Projects/New-Milan-Trade-Fair-Milan*
[Accessed 21 December 2015]

Figure 2.17 Left: L'Oceanografic by Felipe Gabaldón from Spain (Flickr) *[CC BY 2.0 (http://creativecommons.org/licenses/by/2.0)], via Wikimedia Commons*
URL: *https://upload.wikimedia.org/wikipedia/commons/d/d4/L%27Oceanogra fic_%28Valencia%2C_Spain%29_01.jpg*
[Accessed 18 December 2015]

Right: Mapungubwe Interpretation Centre by ©Iwan Baan

Figure 2.18 Left: Inside the Weald and Downland Gridshell by Hugh Chevallier [*CC BY-SA 2.0 (http://creativecommons.org/licenses/by-sa/2.0)], via Wikimedia Commons.*
URL: *https://upload.wikimedia.org/wikipedia/commons/5/59/Inside_the_Weald_and_Downland_Gridshell_-_geograph.org.uk_-_258909.jpg*
[Accessed 16 October 2015]

Right: Trada Pavillion by ©Rambøll
URL: *http://www.grasshopper3d.com/profiles/blogs/trada-pavilion*
[Accessed 9 December 2015]

Figure 3.1 Partly redrawn image after sketches made by J.N-L Durand.
URL: *http://cumincad.architexturez.net/system/files/pdf/8403.content.pdf* [Accessed 10 November 2015]

Figure 3.3 Left: Rendering of Emporia Shopping Centre by ©Wingårdh Arkitektkontor AB.

Right: Emporia Shopping Centre by ©Tord-Rikard Söderström.

Figure 3.5 Mexico City Airport Overview by ©Foster + Partners.

Figure 3.6 Mexico City Airport Interior by ©Foster + Partners.

Appendix A – Calculation of loads

The following calculations have been performed in order to estimate and simplify the loads applied to the canopy in the study project in chapter 4. The loads have been considered in Ultimate Limit State, where the internal stresses and forces (with a load combination factor) is compared to the capacity of the structure.

The glass is assumed to be connected to the steel structure only at the nodes. Therefore the distributed loads, in this case the self-weight of the glass, the wind load and the snow load, are applied as point loads at the nodes.

The load combinations are applied according to *Eurocode SS-EN 1990, Chapter 6.4.3.2, expression 6.10:*

$$\sum_{j\geq 1} \gamma_{g,j} G_{k,j} + \gamma_p P_k + \gamma_{Q,1} Q_{k,1} + \sum_{i>1} \gamma_{Q,i} \psi_{0,i} Q_{k,i} \qquad (A.1)$$

where

$\gamma_{g,j}$	Partial safety factor for permanent load
$G_{k,j}$	Permanent load
γ_p	Partial safety factor for point loads
P_k	Point loads
$\gamma_{Q,1}$	Partial safety factor for primary variable load
$Q_{k,1}$	Primary variable load (snow/wind)
$\gamma_{Q,i}$	Partial safety factor for secondary variable load
$\psi_{0,i}$	Load combination factor for secondary loads
$Q_{k,i}$	Secondary variable load (snow/wind)

Geometric simplifications has been assumed, and the structure has been studied along the middle section shown in the sketches below.

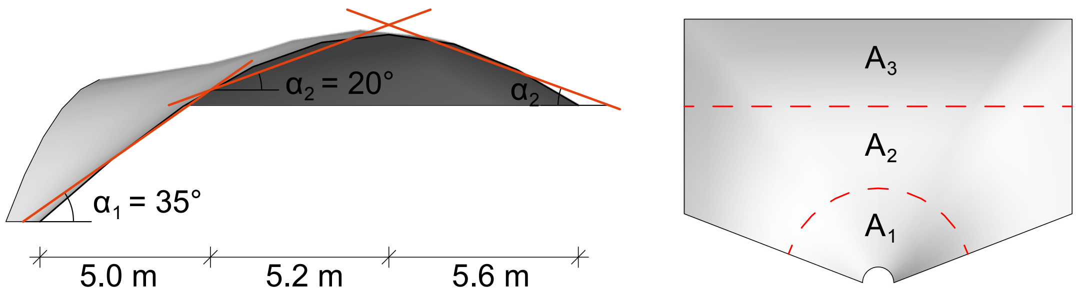

Figure A.1 Geometric simplifications of the structure. It is divided into three loading zones according to the slope of the canopy.

A.1 Self-weight

The self-weight of the steel structure, G_{steel}, is found internally in the FE-program Karamba, using steel grade S235.

$G_{steel} = g\rho_{steel}V_{steel}$ Calculated within Karamba ($\rho_{steel} = 8\,000\ kg/m^3$)

A dead load is added to represent the glass layer, as a uniformly distributed load of:

$$G_{glass} = g\rho_{glass}t_{glass} = 0.147\ kN/m^2 \qquad (A.2)$$

assuming

$\rho_{glass} = 2500\ kg/m^3$ Density of glass
$t_{glass} = 6\ mm$ Thickness of glass panes

A.2 Wind load

The wind load acting on the structure is calculated by multiplying the peak velocity pressure, which depends on the reference height z, with pressure coefficients which depend on the roof angle and wind direction. The structure is assumed to be a kinked duo-pitched roof where the worst case (zone G and J) is assumed for the three zones.

The peak velocity wind pressure is calculated according to *Eurocode SS-EN 1991-1-4*:

$$q_p(z_e) = c_e(z)q_b = 0.468\ kN/m^2 \qquad (A.3)$$

where

$c_e(z) = 1.2$ Exposure factor (Terrain category IV)
$q_b = 0.39\ kN/m^2$ Reference mean velocity pressure (Gothenburg)

The wind is assumed to act on the structure according to four load cases shown in figure below.

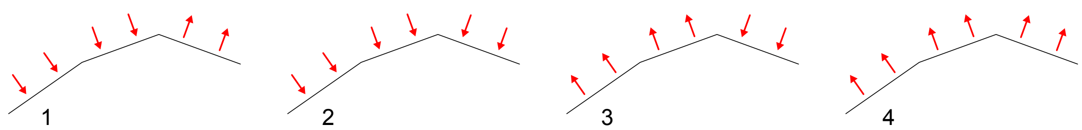

Figure A.2 Load cases of wind acting on the structure

The external wind pressure coefficients, c_{pe}, for duo-pitched roofs are found by interpolating the values found in *Eurocode SS-EN 1991-1-4, Table 7.4a*, presented in Table A.1.

Table A.1 External wind pressure coefficients, c_{pe}

Load case / Zone	1	2	3	4
A_1	0.7	0.7	-0.33	-0.33
A_2	0.37	0.37	-0.77	-0.77
A_3	-0.83	0.0	0.0	-0.83

The wind load is calculated according to *Eurocode SS-EN 1991-1-4, Chapter 5.2:*

$$w_e = q_p(z_e)c_{pe} \qquad (A.4)$$

Table A.2 Wind loads, w_e, on the three zones of the structure [kN/m^2]

Load case / Zone	1	2	3	4
A_1	0.33	0.33	-0.15	-0.15
A_2	0.17	0.17	-0.36	-0.36
A_3	-0.39	0.00	0.00	-0.39

A.3 Snow load

The roof is assumed to be a multi-spanned roof with an adjacent vertical wall. The snow load is calculated according to *Eurocode SS-EN1991-1-3, Chapter 5.1*:

$$S = \mu_i C_e C_t S_k \qquad (A.5)$$

where

μ_i	Shape coefficients
$C_e = 1.0$	Exposure coefficient
$C_t = 1.0$	Thermal coefficient
$S_k = 1.5\ kN/m^2$	Characteristic value of snow on the ground (Gothenburg)

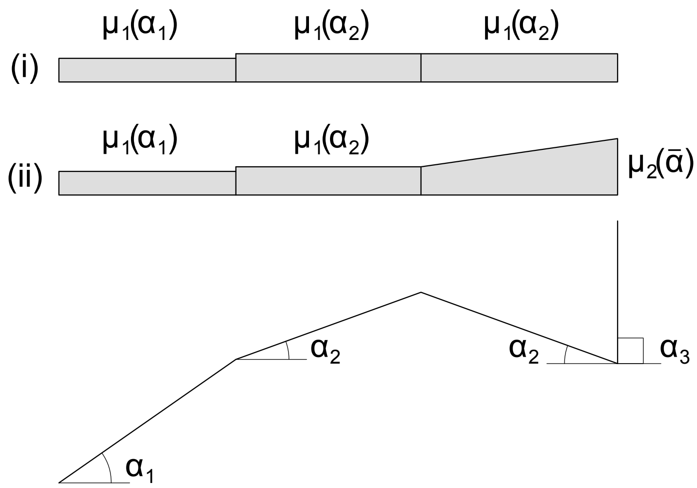

Figure A.3 *Slope and snow load cases for the canopy according to Eurocode SS-EN 1991-1-3, Chapter 5.3.4).*

According to *Eurocode SS-EN 1991-1-3, Table 5.2*, the following snow load coefficients is used:

$\mu_1(\alpha_1 = 35°) = \frac{0.8(60-\alpha)}{30} = 0.67$ since $30° \leq \alpha_1 \leq 60°$

$\mu_1(\alpha_2 = 20°) = 0.8$ since $0° \leq \alpha_2 \leq 30°$

$\mu_2(\bar{\alpha} = 55°) = 1.6$ since $30° \leq \bar{\alpha} = \frac{\alpha_2+\alpha_3}{2} \leq 60°$

At the vertical wall, snow will gather according to load case (ii). For simplicity in calculations, a mean value has been chosen for zone A_3 according to the sketch below:

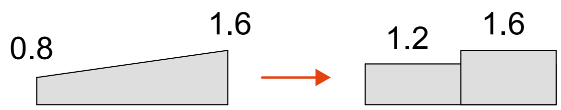

Figure A.4 *Simplification of snow load in zone A_3. The snow load is divided into two zones in A_3.*

A.4 Load combinations

The load combinations according to equation (A.1) is given below. Load combination (LC) 0 is only for the self-weight. LC 1 to 9 have the different wind load cases as the primary variable load, where the dead weight and snow load is counted for as favourable for the upward wind load cases. LC 10-17 have the different snow load cases as the primary variable load. Here, the wind is favourable when having upward direction.

$LC\ 0 \quad 1.35 \cdot (G_{steel} + G_{glass})$

$LC\ 1 \quad 1.35 \cdot (G_{steel} + G_{glass}) + 1.5 \cdot Q_{wind,1} + 1.5 \cdot 0.6 \cdot Q_{snow,1}$ (Unfavourable)
$LC\ 2 \quad 1.0 \cdot (G_{steel} + G_{glass}) + 1.5 \cdot Q_{wind,1}$ (Favourable)
$LC\ 3 \quad 1.35 \cdot (G_{steel} + G_{glass}) + 1.5 \cdot Q_{wind,2} + 1.5 \cdot 0.6 \cdot Q_{snow,1}$ (Unfavourable)
$LC\ 4 \quad 1.35 \cdot (G_{steel} + G_{glass}) + 1.5 \cdot Q_{wind,3} + 1.5 \cdot 0.6 \cdot Q_{snow,1}$ (Unfavourable)
$LC\ 5 \quad 1.0 \cdot (G_{steel} + G_{glass}) + 1.5 \cdot Q_{wind,3}$ (Favourable)
$LC\ 6 \quad 1.0 \cdot (G_{steel} + G_{glass}) + 1.5 \cdot Q_{wind,4}$ (Favourable)

$LC\ 7 \quad 1.35 \cdot (G_{steel} + G_{glass}) + 1.5 \cdot Q_{wind,1} + 1.5 \cdot 0.6 \cdot Q_{snow,2}$ (Unfavourable)
$LC\ 8 \quad 1.35 \cdot (G_{steel} + G_{glass}) + 1.5 \cdot Q_{wind,2} + 1.5 \cdot 0.6 \cdot Q_{snow,2}$ (Unfavourable)
$LC\ 9 \quad 1.35 \cdot (G_{steel} + G_{glass}) + 1.5 \cdot Q_{wind,3} + 1.5 \cdot 0.6 \cdot Q_{snow,2}$ (Unfavourable)

$LC\ 10 \quad 1.35 \cdot (G_{steel} + G_{glass}) + 1.5 \cdot Q_{snow,1} + 1.5 \cdot 0.6 \cdot Q_{wind,1}$ (Unfavourable)
$LC\ 11 \quad 1.35 \cdot (G_{steel} + G_{glass}) + 1.5 \cdot Q_{snow,1}$ (Favourable)
$LC\ 12 \quad 1.35 \cdot (G_{steel} + G_{glass}) + 1.5 \cdot Q_{snow,1} + 1.5 \cdot 0.6 \cdot Q_{wind,2}$ (Unfavourable)
$LC\ 13 \quad 1.35 \cdot (G_{steel} + G_{glass}) + 1.5 \cdot Q_{snow,1} + 1.5 \cdot 0.6 \cdot Q_{wind,3}$ (Unfavourable)

$LC\ 14 \quad 1.35 \cdot (G_{steel} + G_{glass}) + 1.5 \cdot Q_{snow,2} + 1.5 \cdot 0.6 \cdot Q_{wind,1}$ (Unfavourable)
$LC\ 15 \quad 1.35 \cdot (G_{steel} + G_{glass}) + 1.5 \cdot Q_{snow,2}$ (Favourable)
$LC\ 16 \quad 1.35 \cdot (G_{steel} + G_{glass}) + 1.5 \cdot Q_{snow,2} + 1.5 \cdot 0.6 \cdot Q_{wind,2}$ (Unfavourable)
$LC\ 17 \quad 1.35 \cdot (G_{steel} + G_{glass}) + 1.5 \cdot Q_{snow,2} + 1.5 \cdot 0.6 \cdot Q_{wind,3}$ (Unfavourable)

Appendix B – Cross section optimization

The figures below show the result from the process cross section optimization for the other meshes.

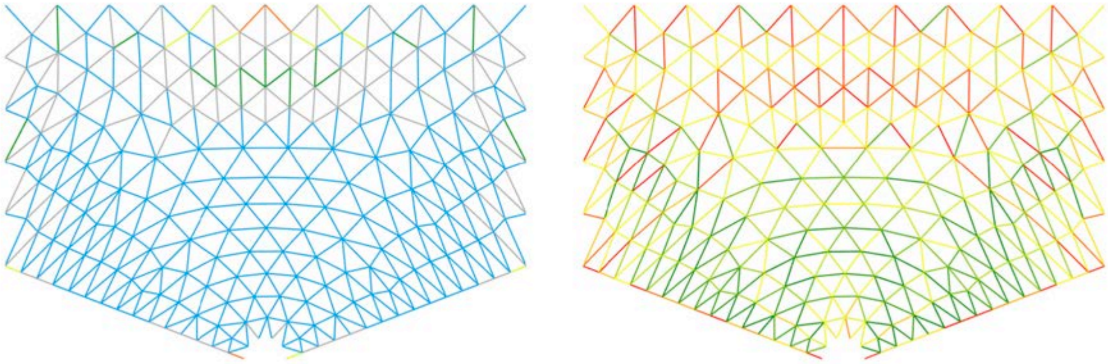

Figure B.1 Cross section layout and utilization for the triangular branched mesh, m_{steel}=4 472 kg (before: m_{steel}=11 870 kg). 62% mass reduction.

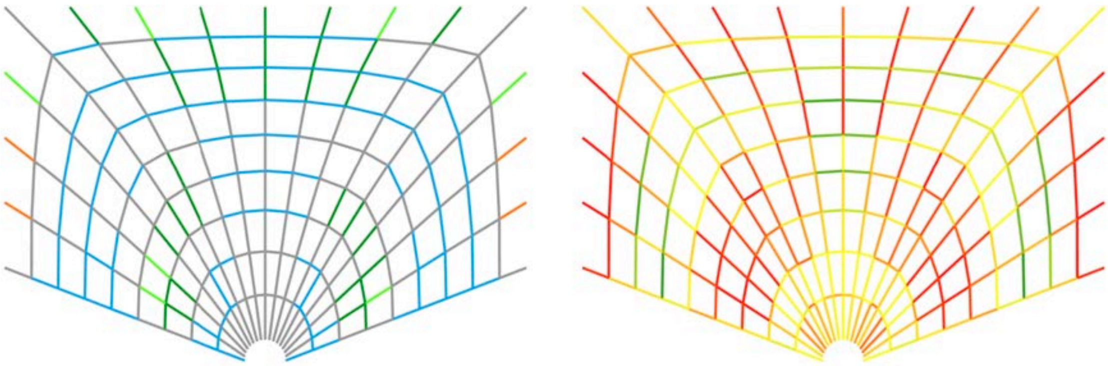

Figure B.2 Cross section layout and utilization for the quadrilateral grid with fixed joints, m_{steel}=6 427 kg (before: m_{steel}=15 184 kg). 58% mass reduction.

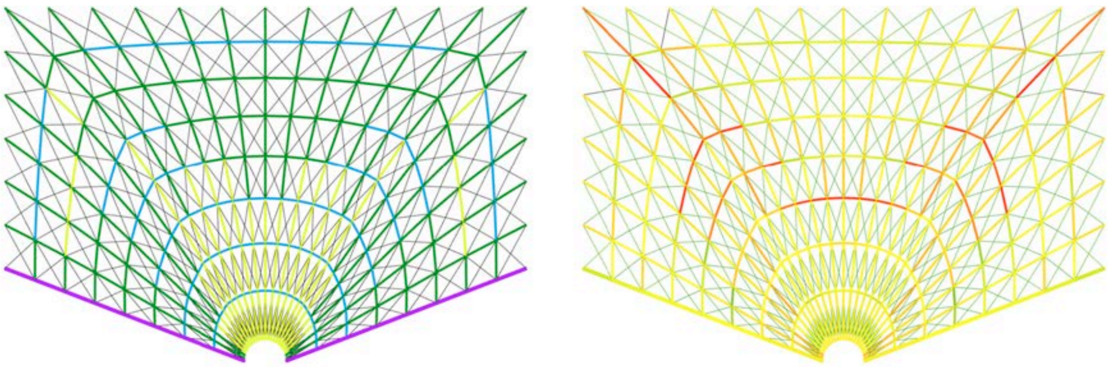

Figure B.3 Cross section layout and utilization for the quadrilateral grid with diagonal bracing, m_{steel}=15 570 kg (before: m_{steel}=27 627 kg). 44% mass reduction.

Table B.1 Division and colour explanation of bars [mm].

Thickness	2.0	4.6	6.3	8.0	9.7	13.6	20.0 (d=190.0)
Colour							
No. of bars (Branch)	423	118	15	-	9	3	-
No. of bars (Quad fixed)	86	153	31	7	-	4	-
No. of bars (Quad diagonal)	108	-	179	-	65	-	16

Appendix C - Reducing number of unique panels

The figures below show the result from the process of reducing the number of unique panels. All grids are assumed to be symmetric, hence the same panels can be laid out on the other side of the symmetry line.

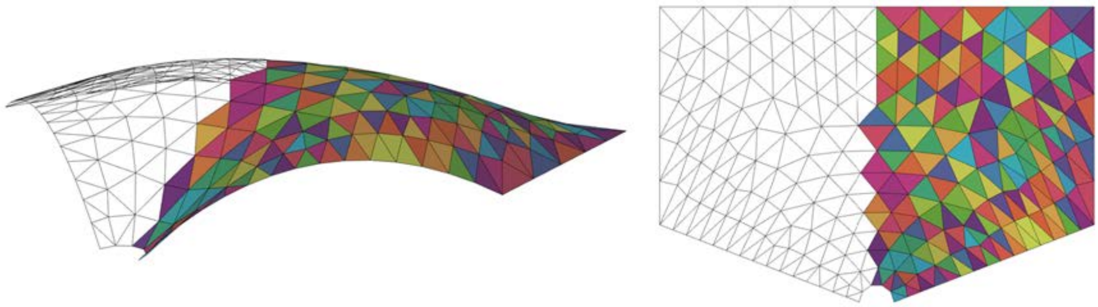

Figure C.1 Triangular branched grid, 172 unique panels (before 194). Deviation=0.01 m. 11% reduction.

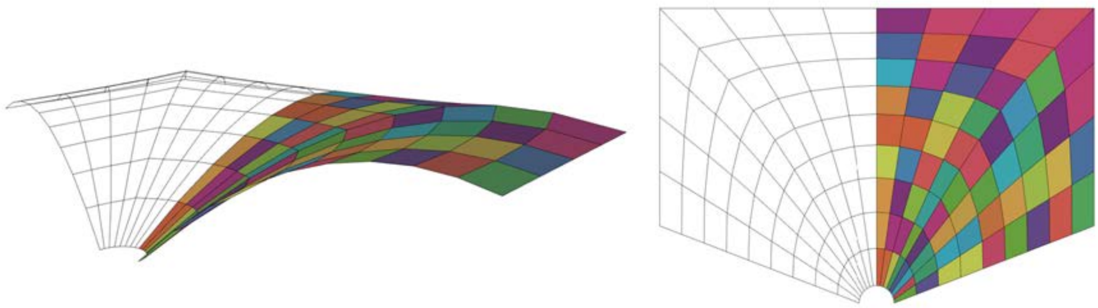

Figure C.2 Quadrilateral grid with fixed joints, 69 unique panels (before 72). Deviation=0.01 m. 4% reduction.

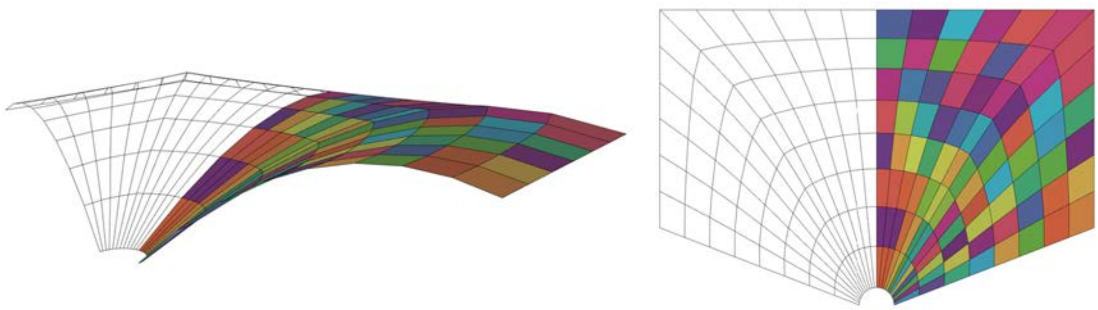

Figure C.3 Quadrilateral grid with diagonal bracing, 90 unique panels (before 96). Deviation=0.01 m. 6% reduction.